European Master
ERASMUS MUNDUS MASTER IN
MEMBRANE ENGINEERING

Universidad Zaragoza
1542

Master thesis project:

Mixed Matrix Membranes (MOFs based) for separation applications

STUDENT: ALINA KUDASHEVA

SUPERVISOR: JOAQUIN CORONAS

UNIVERSITY OF ZARAGOZA

June 2013

Acknowledgement

I would like to express my sincere gratitude to my advisor Prof. Joaquin Coronas for the continuous support of my research, for his excellent guidance, patience, and providing me with an excellent atmosphere for doing research. Besides my advisor, I would like to thank to Carlos Tellez for the useful comments, remarks and engagement through the learning process of this master thesis. Also I am grateful to Sara Sorribas and Beatriz Zornoza for their help, advices and support in completing this project and generally my stay in University of Zaragoza. I would also like to thank all of the members of the CREG laboratory for the friendship and nice working environment.

This research project has been financially supported by the Spanish Ministry of Economy and Competitiveness (MINECO, MAT2010-15870), as well as the Regional Government of Aragón (DGA) and the European Social Fund.

Additionally, I would like to thank to the EM3E Master in Membrane Engineering (www.em3e.eu) for accepting me as candidate for EM3E program and giving me the opportunity to grow as a specialist.

The EM3E Master is an Education Programme supported by the European Commission, the European Membrane Society (EMS), the European Membrane House (EMH), and a large international network of industrial companies, research centres and universities.

The EM3E education programme has been funded with support from the European Commission. This publication reflects the views only of the author, and the Commission cannot be held responsible for any use which may be made of the information contained therein. Translation of this phrase in all EU languages.

Content

List of figures

List of tables

List of abbreviations

ATR-FTIR - Attenuated Total internal Reflection Fourier Transform Infrared spectroscopy
BET – Brunauer Emmett Teller
DSC – Differential Scanning Calorimetry
MMM – Mixed Matrix Membrane
MOF – Metal Organic Framework
MIL - Materials Institute Lavoisier
PV – PerVaporation
SEM – Scanning Electron Microscopy
TGA - Thermo Gravimetric Analysis
Tg – Glass Transition Temperature
ZIF – Zeolitic Imidazolate Framework
UV – Ultra Violet

Abstract

This work explores the use of molecular sieves such as Metal Organic Frameworks (MOFs) and ordered mesoporous silica spheres in the fabrication of Mixed Matrix Membranes (MMMs). Since application of MMMs in liquid separation is not well discovered yet, the prepared MMMs were applied in dehydration of alcohol via pervaporation. In particular, the mixture of interest was water/ethanol solution due to its azeotropic composition and therefore difficulties in separation. Ordered mesoporous silica spheres of different sizes and various types of MOFs were introduced into a polymer matrix at different loadings in order to study the effect of the fillers on membrane performance.

1. Introduction

Nowadays the researches attention is focused on new technologies in order to improve production performance and reduce costs. In separation processes membrane technology has been seen to offer many advantages over existing competing technologies such as "higher selectivity, lower energy consumption, moderate cost to performance ration and compact modular design" [1].

Pervaporation is a technology combining membrane permeation and evaporation for molecular-scale liquid separation. This process is widely used in separation of azeotropic mixtures, close-boiling mixtures and for the recovery of small quantities of impurities. Pervaporation has several advantages comparing to conventional separation processes (e.g. distillation, adsorption, etc.). Firstly, pervaporation is based on the differential transport of penetrants through the membrane instead of the vapour-liquid equilibrium, and thus has a superior separation efficiency [2]. Secondly, this process avoids cross-contamination by the third component in the case of separation azeotropic mixtures. Traditionally the way to separate azeotropes and allow them to be completely dehydrated is to add additional chemical such as cyclohexane to the mixture before distillation. However the use of cyclohexane adds another impurity to alcohol and can never entirely be removed, and thus rendering the alcohol product unsuitable for applications where high purity alcohol is required [3]. Thirdly, pervaporation process outperforms conventional technologies in terms of energy saving because only the component penetrating through the membrane consumes the latent heat [4]. Additionally, compactness and simplicity in module fabrication and in system process control are strong points of this technology.

The bigger difference between water and the solvents in membrane solubility makes dehydration of alcohols the most feasible application for pervaporation [5]. Pure or absolute ethanol

is widely used in many applications, for instance, as a fuel additive, as a solvent in the laboratories and as a cleaning agent, it is also used in UV and visible light spectroscopy as the solvent for the samples, also ethanol has applications in pharmaceutical, perfumery and wine industries etc.

The efficiency of the pervaporation process depends mainly on the properties of the polymers used to prepare the membrane. Hence, designing membrane structure with a high permeation rate and separation factor is an important issue. The performance of polymeric membranes used in pervaporation process is limited by an upper bound trade-off line, which demonstrates a strong inverse relationship between permeability and selectivity of the membrane (polymers that are more permeable are commonly less selective and vice versa) [6]. Therefore it is very important to develop membranes with high pervaporation performance.

Nowadays, in order to improve performance, there is a huge interest in synthesizing new materials and modifying the existing membrane materials for better separation performance. A strong improvement of permeability can be expected if a porous additives, which has a pore diameter larger than kinetic diameter of one component of the mixture but smaller than the other one, could be applied to the organic polymer. The solid (dispersed) phase that is incorporated into a polymer phase forms a mixed matrix membrane (MMM). MMMs are highly potential composite materials that may possibly overcome the challenges faced by the membrane technology today [7]. As additives into polymer phase, metal organic frameworks (MOFs) can be used. MOFs are relatively a new family of nano porous materials that are produced from metal ions or clusters linked by organic molecules [8]. Their incorporation into membranes is a promising application because MMM could combine the molecular sieving effect of MOFs and process ability of the base polymers. MOFs play an important role in membrane technology because of their high porosity and easy tunability of their pore size and shape from microporous to mesoporous scale by changing the connectivity of the inorganic part and the nature of organic linkers [9]. Therefore, they could be readily scaled up for industrial applications using the established fabrication techniques for polymeric membranes.

There is a limited number of the researches, focused on the liquid separation with MMMs containing MOFs, published at present. Only results of the separation of water/alcohol mixture with MMMs based on ZIF-8 [10, 11] are available. Therefore in this study we are one of the first who discovers the influence of different molecular sieves such as MOFs and ordered mesoporous silica spheres on the MMM separation performance in liquid separation.

1.1. Challenges and proposal

The main challenge in the case of separation of ethanol-water mixture is a low permeability. Water activity coefficient and partial vapour pressure in the ethanol-water system are much lower than those in the other alcohol-water mixture such as butanol-, propanol- or isopropanol-water systems, and hence the former has a lower driving force of water across the membrane. This leads to a lower flux of the water/ethanol system [12]. To overcome these limitations we propose to use MMMs containing MOFs that will turn dense membrane into the nanoporous membrane. The selected for this study fillers have pore sizes in the range of 0.3-3 nm that will allow to water molecules to pass through the membrane and selectivity of the membrane will be based on distinguishing the molecules size of two mixture components which are water and ethanol.

1.2. Aim and objectives

The overall aim of this research is to synthesize mixed matrix membranes (MMM) using a polymer material and various porous crystalline solids. This work aims are to improve the mass transport properties of polymeric membrane through addition of porous crystalline solids and to balance membrane separation performance i.e. selectivity and permeability. These can realised through the following objectives:

- To successfully synthesize and characterize micro and nanoparticles of the following fillers: MOFs ZIF-8, MIL-101 and HKUST-1, MCM-41 ordered mesoporous silica spheres and ordered mesoporous silica-(ZIF-8) core-shell spheres, obtaining comparable powder surface areas to those reported in the literature.
- To successfully synthesize and characterize MMMs with various loadings of the fillers.
- To test the membrane separation performance in dehydration of the water/ethanol mixture via pervaporation and investigate the membrane long term performance and stability.
- To demonstrate the importance of proper material selections.
- To fundamentally understand the dehydration and separation mechanisms at molecular level.

1.3. Strategies for membrane development

To develop suitable synthetic membranes for pervaporation two strategies can be considered. One is the molecular design of material chemistry of dense-selective layer materials with desired physicochemical properties such as inherent solubility, selectivity and diffusivity. And the other strategy is macromolecular engineering of membrane structure of the dense-selective layers with desired morphology and defect free characteristics [2]. As a result, synergistic balance between diffusion selectivity and sorption selectivity as well as high permeability with desired separation performance can be achieved. In order to develop membranes with desired physicochemical properties and with long term stability the proper selection of materials is required. To obtain membranes free of defects, the effect of typical membrane processing conditions on the structure and interfacial morphology should be investigated.

2. Material selection

2.1 Polymer selection.

Nowadays there are many types of the polymer materials that can be used in membrane separation. A polymer to be effective in separation process must be chemically resistant, mechanically and thermally stable and include a high PV flux (which determines the productivity) and high selectivity (high development of the material) [13]. In the case of dehydration of water/ethanol mixture there is a low concentration of water that needs to be separated from the mixture, hydrophilic membranes are generally used as they preferentially allow water to diffuse through, resulting in production of permeate with a high water concentration and dehydrating ethanol in the retentate side [3].

For water selective membranes, the most important factor responsible for the separation is the specific interaction between water and the polymer. Using polymers, which contain specific groups like active centers which are capable of strong interactions with water, it is possible to have high selectivity membrane. Higher sorption selectivity in the polymer can be achieved if the energy of the interaction between water and the active center is higher. In this respect, polymers with hydrogen bonding and ion-dipole interactions are expected to exhibit the highest selectivity, since these are the most energetic interactions. There are two types of interaction [14]:

- Hydrogen bonding interaction.

The hydrogen bonding interactions are mainly possible in polymers containing hydroxyl group such as polyvinyl alcohol (PVA**),** polymers containing amide/imide groups**,** polymers containing

carboxylic groups (cellulose acetate, polyvinylacetate etc.) and other groups which are capable to form strong hydrogen-bonding with water.

- Ion-dipole interactions.

These interactions are mainly present in polymers containing fixed charged ionic groups, which can strongly interact with water. Some examples of such materials are polymers containing partially quarternized ammonium basics, various ion-exchange membranes like Nafion and polyelectrolyte complexes (chitosan, cellulose sulfate, etc.)

For this study polyimide such as Matrimid 5218 (supplied by Huntsman Advanced Materials) was chosen due to its strong interaction with water. Polyimide has polar carbonyl groups which are capable of forming hydrogen bonding with water as shown in the Fig.1 [15]. Shimidzu and co-workers believed that the polar groups in the membrane matrix, responsible for the membrane hydrophilicity, act as fixed carriers for mass transport in the membrane [5].

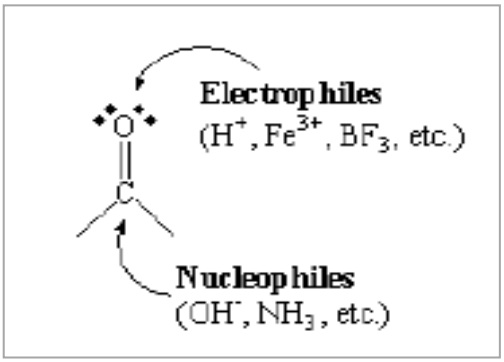

Figure 1. Possible reactions at the carbonyl group [16].

When compared to most other organic or polymeric materials, polyimides exhibit an exceptional combination of thermal stability (>500°C) and mechanical strength. Polyimides are rigid with high-melting point, high glass transition temperature [17]. Glassy polymers such as Matrimid 5218 are better than rubbery polymers because of their rigid structure, adhesion between the polymer phase and the external surface of the particles is a major problem when glassy polymers are used in the preparation of mixed matrix membranes [18]. Also the selectivity of membranes based on Matrimid is associated to their rigid molecular chains, due to strong intermolecular bonds between carbonyl group and the nitrogen atom, imposing major constrains to rotation and mobility of the polymeric structure [19]. Also Matrimid has a high resistance to organic solvents [20]. And this was an additional criteria of selecting the base material for the membrane.

2.2 Filler selection.

For mixed matrix membranes a perfect interaction between the two components is highly important in order to achieve optimized separation properties of the hybrid material [21]. Therefore it is necessary to properly select the molecular sieve material in order to successfully fabricate mixed matrix membrane. An ideal system would be one where the sieve has a stronger affinity for the polymer than the solvent, while polymer has a stronger affinity for the sieve surface than the solvent [22].

Based on the pore size there are four types of membranes which are (1) dense membrane with pore diameter (Øp) less than 0.5 nm, (2) microporous: $0.5 < Øp < 2$ nm, (3) meso-porous: $2 < Øp < 50$ nm, and (4) macro-porous: $Øp > 50$ nm [23]. Micro-porous membranes can be highly selective for water [24]. Hence to prepare micro-porous membranes we have selected the fillers with the pore size in the range of 0.5-2 nm. In order to highly improve the permeability of the membrane we have also chosen the mesoporous fillers with the pore size in the range of 2-4 nm. Ordered mesoporous silica spheres and various types of MOFs have been selected for this study and their textural properties are presented in the Table 1 where the values of BET specific surface areas and the particles size refer to this study. And the SEM images of prepared MOFs and silica spheres can be seen in the Fig.2.

Table 1. Textural properties of the different filler materials.

MOFs type	Pore topology	Pore diameter, nm	S BET, m^2/g	Particle size
ZIF-8	cage/window	1.16 / 0.34	1214	170 ± 20 nm
MIL-101	cage/window	2.9 / 1.2 3.4 / 1.6	2074	180 ± 30 nm
silica spheres MCM-41	hexagonal symmetry	2.7-3; ~15	939	3.1 ± 0.30 μm
silica spheres MCM-41	hexagonal symmetry	2.7-3	923	530 ± 140 nm
HKUST-1	cage/window	1.1 / 0.6	-	680 ± 170 nm
HKUST-1	cage/window	1.1 / 0.6	1925	16.0 μm
Silica-(ZIF-8) core-shell spheres	core (hexagonal)-shell (cage/window)	(2.7-3; ~15)-(1.16/0.34)	1005	4.3 ± 0.6 μm

ZIF-8 is MOF that made from linking of zinc (II) cations and 2-methylimidazole anions, giving a sodalite topology with a pore cavity of 11.6 Å and a theoretical pore aperture of 3.4 Å [25]. Due to its organic nature, ZIF-8 easily adhere to the host polymer matrix [26] and provide the homogeneous dispersion and as a result a homogeneous hybrid membrane, which can be seen in the section 4.3. This MOF is chosen due to its right size for separating water and alcohols, and might also increase diffusivity of water molecules. However, the high hydrophobicity of the material may favour the sorption of alcohols, hence the effects of adding ZIF-8 for the pervaporation dehydration of alcohols remains unclear. ZIF-8 nanoparticles were prepared as described in the literature [27].

MIL-101 is a crystalline mesoporous material: Chromium (III) Terephthalate (3D-$[Cr_3O(BDC)_3(F,OH)\text{-}(H_2O)_2]$). The MIL-101 materials have a zeotype crystal structure comprising two kinds of cages with free internal diameters of 29 and 34 Å, accessible through microporous windows of 12 and 16 Å [28]. MIL-101 was chosen because it is one of the most water-stable carboxylate MOFs which has a huge pore volume and surface areas [29]. MIL-101 nanoparticles were synthesized as described in the literature [9].

MCM-41 type silica spheres is a mesoporous material that have some unique properties such as mechanical and thermal stability, facility of chemical functionalization and well defined mesoporous array and porosity [26]. Silica spheres have two particle size distribution which are 2.7-3 nm and 15 nm [30]. Due to mesoporosity of silica particles, and taking into account that the cross sectional areas per chain of the most selective synthetic polymers are around 1 nm^2 or less, the polymer chains are able to penetrate into the mesoporosity of the filler to give rise to a real homogeneous nanoporous composite, hence render a good adhesion between the fillers and polymer. [13]. For this study two types of MCM-41 silica spheres were used which differ from each other in the size of the particle. The size of prepared spheres were 3.1 μm and 530 nm, the synthesize procedure was performed as described in the literature [30] for micro size silica spheres and as was described by Manzano et al. [31] for nano size silica spheres..

Ordered mesoporous silica–(ZIF-8) core-shell spheres is a composite made of mesoporous silica spheres MCM-41 and ZIF-8. The mesoporous spheres were used as a core and hydrophobic microporous ZIF-8 crystallites formed the shell that controls the entrance of guest molecules into the hydrophilic mesopores. With introducing these core-shells in the polymer phase we expect an enhancement in selectivity since the ZIF-8 shells can distinguish guest molecules based on their size and then silica spheres, that are hydrophilic, will perform the permeation of the molecules that are passed through the shells. The textural properties of these two materials are described above, the average particle size of the core-shells spheres is 4.3 μm and their synthesize procedure is described in the literature [27].

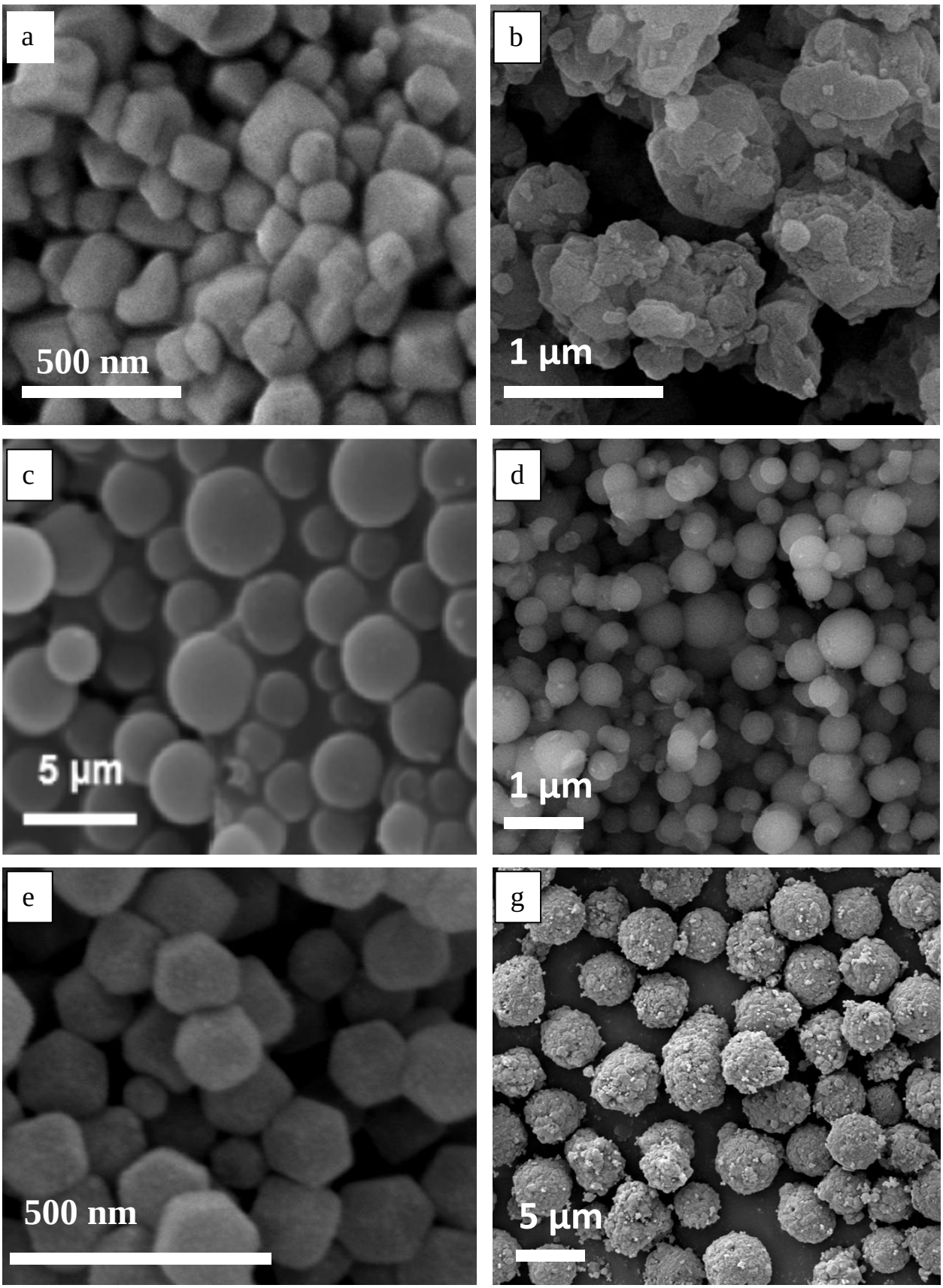

Figure 2. SEM images of the prepared molecular sieves: (a) MIL-101; (b) HKUST-1 (size 680 nm), (c) silica spheres MCM-41 (size 3.1µm), (d) silica spheres MCM-41 (size 530 nm); (e) ZIF-8; (g) silica-(ZIF-8) core-shell spheres.

HKUST-1 is MOF, which is also called [$Cu_3(BTC)_2$], is composed of copper dimers coordinated to the oxygen atoms of benzene-1,3,5-tricarboxylate (BTC) linkers, forming a regular porous network with a high specific pore volume [32]. HKUST-1 is the framework that contains micro pores 1.1 nm which are accessible through small apertures of 0.6 nm that allow penetration of guest molecules and also shape and size selective separations. For this study HKUST-1 particles of two sizes were used: 16 μm (was supplied by Sigma Aldrich) and 680 nm (was synthesized in our laboratory).

All the fillers mentioned previously were chosen for the preparation mixed matrix membranes because it was assumed that all of them would facilitate the preparation of highly homogeneous membranes. Most of the selected molecular sieves are hydrophilic because using the hydrophilic fillers reduces the required activation energy for attracting water molecules and thus water permeation flux through mixed matrix membrane [15].

In addition to material selection, research in mixed matrix membrane also covers membrane formation technique, characterization and performance evaluation. Membrane formation includes the solution preparation, surface treatment, casting process and post treatment. Characterization and performance evaluation are important for better understanding of the relationship between membrane morphology and its transport properties.

3. Experimental

3.1 Membrane preparation.

To fabricate a mixed matrix membrane (MMM), material selection for polymer matrix as well as filler material are the key aspects in order to have a membrane with good chemical strength and excellent separation performance. Among the materials that can be utilized for pervaporation, polymers are preferred due to their compactness, ease of fabrication and scale-up, high energy efficiency and lower capital costs.

The first step of our experiment was to fabricate the plain polymeric membrane for the purposes of comparison with those containing increased amounts of molecular sieves. For the preparation of neat polymeric membranes, initially polymer was dried overnight (at 180 °C) to remove any moisture present and then dissolved in a solvent such as chloroform in the ratio 90:10 wt% (solvent:polymer). Chloroform is able to fully dissolve the polymer, allowing good viscosity of the casting solution.

To fabricate MMMs (Fig.3), the synthesized molecular sieves were dispersed in chloroform in an ultrasonic bath for 20 minutes and stirred after overnight to complete dispersion. The polymer

was added then and the solution was stirred magnetically at room temperature for 24 hours. Before the casting of solution 3-4 intervals of sonication for 20 minutes were performed in order to obtain a well dispersed solution. Subsequently, homogeneous solution was cast on a Petri dish and left overnight partially closed to slow down the evaporation of solvent. The last step of membrane preparation was thermal treatment of membranes in the vacuum oven at temperature 180 °C and pressure 10 mbar to ensure the solvent evaporation. The glass plate was put into a vacuum oven and the membrane was left uncovered [33].

The filler loading in the membrane was calculated as following formula:

$$\text{Particle loading, wt\%} = \frac{particle\ weight}{particle\ weight + polymer\ weight} \times 100.$$

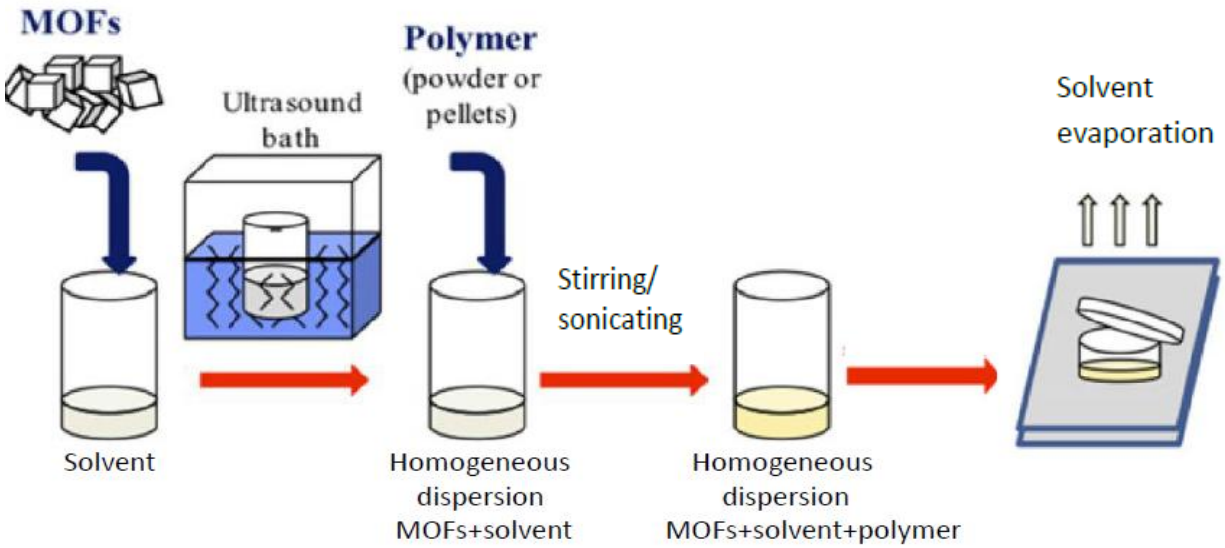

Figure 3. General scheme for the fabrication of MMMs containing MOFs [34].

3.2 Pervaporation experiment.

In pervaporation, the feed solution of 10/90 wt% of water/ethanol was in direct contact with the membrane and pervaporation was performed at two different temperatures: 40 and 55 °C. The testing membrane was placed in a stainless steel permeation cell with an effective surface area of 12 cm^2. The membrane downstream (permeate) side was evacuated using a vacuum pump (pressure 38 - 45 mbar). The steady state was achieved by running the experiment for about 12 hours[1]. The

[1] The steady-state mass transport regime depends on several parameters, i.e., upstream pressure, downstream pressure, temperature and film thickness.

permeate vapour was trapped and condensed by a glass cold trap immersed in liquid nitrogen. The condensed permeate was warmed up to room temperature and then the permeation rate was determined by measuring the weights of permeate by a Mettler Toledo balance. Finally the compositions of permeate were analyzed by gas chromatography. The membrane performance in pervaporation experiments was studied by calculating the total flux and separation factor as described in the Annex 8-A.

A laboratory scale pervaporation set up was used to carry out the pervaporation experiments, as shown schematically in Fig.4. The permeation cell was placed in the oven in order to perform experiments at desired temperatures.

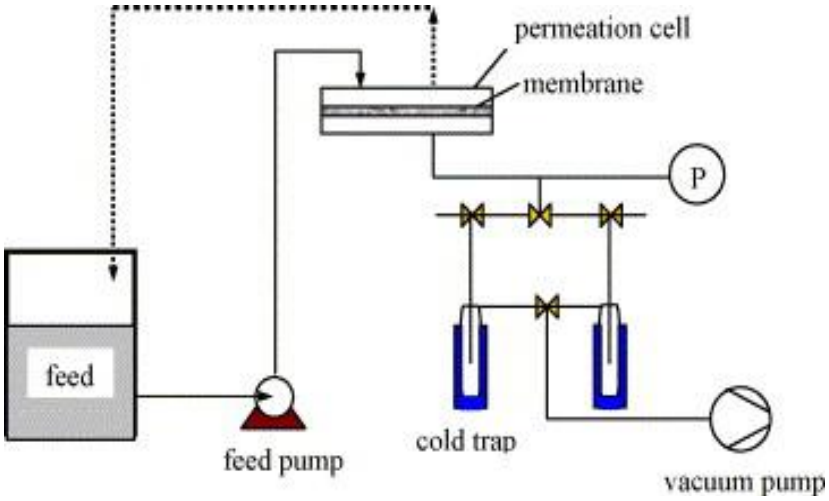

Figure 4. Schematic diagram of pervaporation apparatus [35].

3.3 Characterization

A number of characterization techniques were used to determine the following properties:

- the composition of the permeate (Gas Chromatography);
- the geometrical characteristics and the morphology of the MMMs (Scanning Electron Microscopy, SEM);
- the glass transition temperature (Differential Scanning Calorimetry, DSC);
- the thermal stability of the membranes (Thermo Gravimetrical Analysis, TGA);
- the chemical structure changes of membranes (ATR-Fourier Transformed Infrared Spectroscopy, FTIR);
- the degree of swelling of the membranes (Swelling test).

All aforementioned techniques are described in details in the Annex 8-B.

4. Results and discussion

All the additives that were used in the preparation of the MMMs were selected for a specific purpose, based on their nature and their pore size. In this chapter the effect of molecular sieves, embedded into polymer matrix, on the membrane performance will be shown. Also the influence of high filler loadings on the membrane separation properties will be discussed.

4.1 Membranes based on pure Matrimid

From the results given in the Table 2 and the Fig. 5 we can see that with increasing the temperature from 40 °C to 55 °C the total PV flux increases. It is well known that increased operating temperature enhances the thermal mobility of the polymeric chain and also leads to a decrease of liquid viscosity, consequently the diffusion rate of the permeating molecules is significantly increased. In the other words, considering the driving force of the PV process, the increase of the chemical potential difference in terms of the temperature difference leads to the flux increase [36].

Table 2. Influence of operating temperature on PV performance.

Temperature, [°C]	Total permeate flux, [kg/(m^2·h)]	Separation factor
40	0.19 ± 0.01	317 ± 25
55	0.24 ± 0.03	260 ± 28

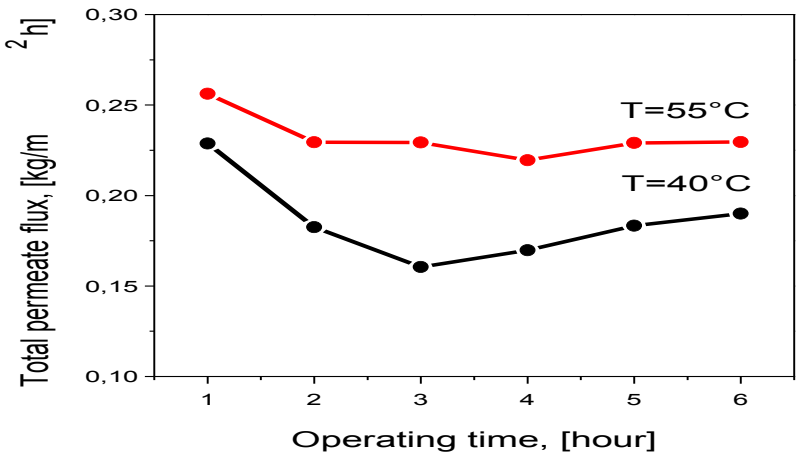

Figure 5. Total PV flux versus operating time at 40 and 55 °C.

However a decrease in selectivity was observed with increasing the temperature. According to the free volume theory [37] an increase in temperature can increase the thermal motion of the polymer chains and generate more free volume in the polymer matrix to facilitate absorption and diffusion of permeate in an organic membrane. The increase in the free volume makes the membrane more permeable but less selective to the permeation of the permeating components, which leads to a higher permeation rate and a lower separation factor.

The experiments showed higher permeation and faster steady state achievement at 55 °C, therefore it was concluded to set up the operating temperature at 55 °C for the rest of the membrane samples.

4.2 Influence of the membrane fabrication technique on the polymer-filler contact. Effect of interfacial defects on the membrane performance.

Because of the difference between the polymer and inorganic phase properties and also aggregation tendency of the fillers, the fabrication technique of the MMMs is a very important step. An ideal MMM is a membrane that is free of defects and has a good polymer-filler interaction. To achieve this good polymer-filler contact and to see how fabrication techniques influence the overall membrane properties, we have prepared two MMMs containing MCM-41 silica spheres (average particle size 3.1 μm) by two different techniques. For the convenience of the reader we would call them case (a) and case (b).

MMM containing silica spheres case (a) was prepared by technique described in the section 3.1. The difference of preparation of MMM containing silica spheres case (b) compare to case (a) is only the step of the solvent evaporation. In the case (b) during solvent evaporation the membrane was completely covered with a glass Petri dish while in the case (a) the membrane was only partially covered. Covering the film provides a more controlled solvent evaporation, also it prevents dust and other particulate matter from falling on the surface of the film. According to Moore and Koros, uncontrolled evaporation leads to defects such as rigidified polymer layer formation around the particles. They have attributed the formation of this rigidified polymer layer to stresses which arise during membrane formation due to solvent evaporation [38].

The results of this study are depicted in the Table 3 and (Fig.6) from where we can see that controlled evaporation of the solvent during membrane fabrication results in a good polymer-sieve interaction and hence in improved membrane permeability.

Table 3. Comparison of PV performance of MMMs prepared by different methods.

Membrane	Filler content, wt%	Total permeate flux [kg/(m^2·h)]	Separation factor
Case (a)	12	0.13	525
Case (b)	12	0.32	206

As it can be seen in the Fig.6 (b) there was a good polymer-sieve interface, probably there were uniform stresses during solvent evaporation resulting in good interfacial adhesion and reduction in free volume near the fillers surface, also known as polymer rigidification [18]. In the case (a) it might be possible that the stress directions were not uniform around the particles surface and thus it may lead to the formation of strongly rigidified layer of polymer around the filler. As a result the preparation of membranes with the same loading of silica spheres but with different solvent evaporation rates leads to the different values of the PV flux and separation factor.

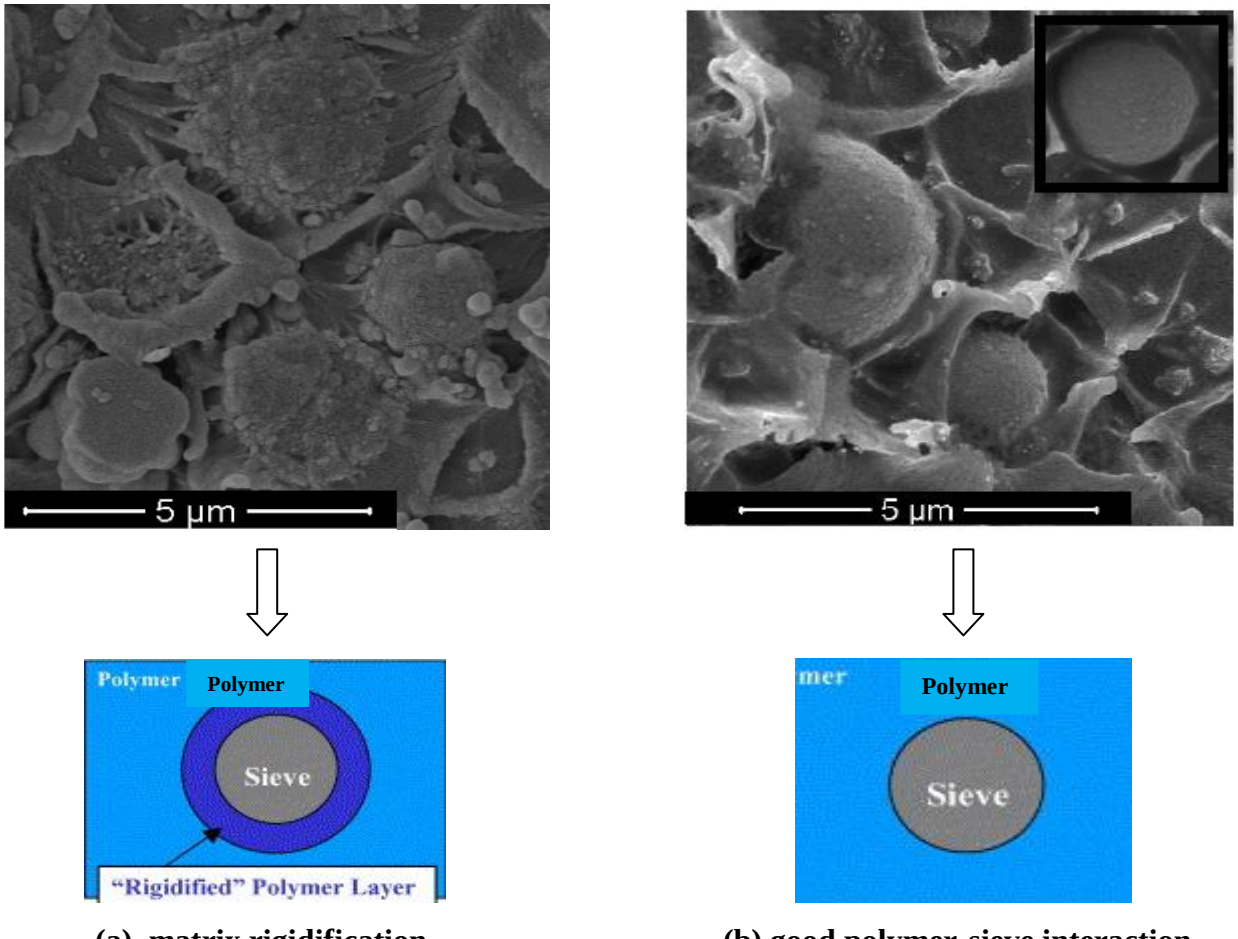

(a) matrix rigidification **(b) good polymer-sieve interaction**

Figure 6. Cross section SEM images of MMMs containing 12 wt% of silica spheres MCM-41.

With a controlled evaporation of solvent the membrane PV flux was more than twice higher but separation factor was much lower comparing to those values of membrane prepared with uncontrolled solvent evaporation. A comparatively high separation factor (case a) can be attributed to the fact that ethanol molecules, which are bigger than water molecules, hardly can pass through the rigidified polymer layer.

From this study we can conclude that it is better to completely cover membrane with glass plate during the casting in order to obtain a good polymer-filler interface and as consequence improve membrane flux without sacrifice in separation factor. Therefore all the membranes for pervaporation experiment were prepared appropriately.

4.3 Effect of the different fillers and their different loadings into polymer on PV performance.

4.3.1 Mixed matrix membranes containing 12 wt% of various fillers.

For the pervaporation experiment MMMs were prepared with addition of 12 wt% of the following fillers: mesoporous silica spheres MCM-41, MIL-101, ZIF-8 and ordered mesoporous silica-(ZIF-8) core-shell spheres. The values of the total permeate flux and separation factor for the neat Matrimid membrane are based on the results of four tested membranes. Table 4 presents the average of those results. In order to compare pervaporation performance of all the membranes that contain 12% of the fillers, Table 4 also includes the results of the MMM containing silica spheres case (b) that was described in the section 4.2. The steady state achievement of the membranes versus time can be seen in the Annex C (Fig.17).

For these experiments only one MMM was prepared with the use of hydrophobic MOF which is ZIF-8, the rest of the membranes contain hydrophilic fillers. The membrane that contains ZIF-8 did not show an enhancement in PV flux while the separation factor was increased from 260 to 386 comparing to membrane based on neat Matrimid. This is due to the fact that water molecules are much smaller than ethanol molecules, the kinetic diameters of water and ethanol are 0.29 nm and 0.43 nm [12] respectively while the ZIF-8 aperture size is 0.34 nm. Thus, in principle, ethanol molecules hardly could pass through the membrane. In addition, the SEM studies (Fig.7 d) shows good compatibility of ZIF-8 with Matrimid and we expected that the higher loading of this MOF into polymer may improve the PV flux.

Table 4. PV performance of MMMs containing 12 wt% of various fillers.

Membrane	Filler type	Flux, [kg/(m^2 h)]	Separation factor
Neat Matrimid	no	0.24 ± 0.03	260 ± 28
MMM	Silica-(ZIF-8) core shell	0.16	115
MMM	MIL-101	0.21	709
MMM	ZIF-8	0.24	386
MMM, case (b)	MCM-41 spheres (size 3.1 μm)	0.32	206
MMM	MCM-41 spheres (size 530 nm)	0.44	229

Some of the MMMs have lower permeability comparing to the neat Matrimid membrane, for instance MMM-(MIL-101) and MMM-(silica-(ZIF-8) core-shell spheres. In the case of MMM containing MIL-101, the polymer-MOF contact was quite good (Fig.7 e) without any defects and as a result the separation factor was improved from 260 to 709 compared to the neat Matrimid membrane. However the PV flux was not enhanced most probably due to the fact that solubility of water is much higher than solubility of ethanol and as consequence due to highly hydrophilic nature of MIL-101 the adsorption of water was very high resulting in low diffusivity.

The MMM that contain silica-(ZIF-8) core-shell spheres not only did not improve permeability, but even had total PV flux much lower than flux of the membrane with ZIF-8 only. The SEM images of the cross section of membrane containing core-shell spheres are presented in the Fig.7 (c), from where it can be seen that actually ZIF-8 particles surround the silica spheres with diameter size around 3.1 μm and hence their interaction with polymer phase forms microcomposite. Whereas membrane containing only ZIF-8 (Fig.7 d) with particle size around 171 nm is a nanocomposite. Thus interface area of ZIF-8 with the polymer is higher than in the case of the silica-(ZIF-8) core-shell spheres. And this tendency can be seen in the Table 5 as well, where the glass transition temperature (Tg) of MMM–ZIF-8 is much higher than Tg of MMM-silica-(ZIF-8) core-shell spheres.

The best results in terms of PV flux showed MMMs that contain hydrophilic mesoporous MCM-41 silica spheres (size 530 nm). Even if the dispersion of silica spheres of two different sizes (3.1 μm and 530 nm) leads to a homogeneous membranes in both cases (Fig.7 a and b), it can be clearly seen in the Table 4 that the use of smaller silica spheres in membrane preparation leads to a better membrane performance, i.e. enhancement of PV flux without significant changes in separation factor. Hence for the further experiments we decided to use nano size silica spheres MCM-41. The results of SEM characterization of the MMMs with higher silica spheres loading will be presented and discussed in the separate study (section 4.3.4).

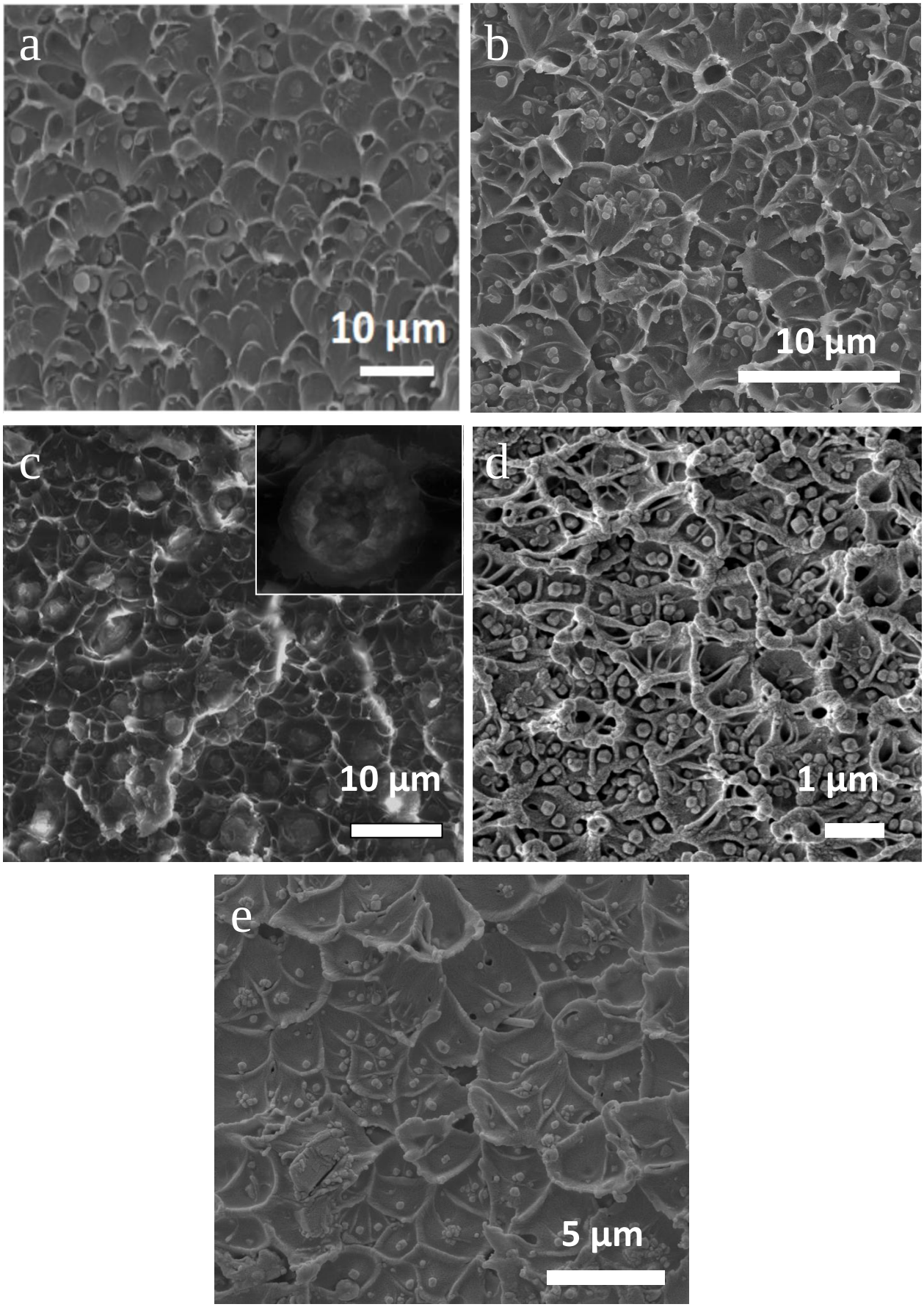

Figure 7. SEM cross section images of MMMs containing 12 wt% of: (a) silica spheres MCM-41 (3.1 µm); (b) silica spheres MCM-41 (530 nm); (c) silica-(ZIF-8) core-shell spheres; (d) ZIF-8; (e) MIL-101.

The DSC characterization technique provided with values of glass transition temperature of all the membranes that contain 12 wt% of molecular sieves (Table 5). Tg values increase due to the presence of fillers within polymer matrices. It can be attributed to the inhibition of polymer chain mobility near the polymer-filler interface by their attachment to the filler or the polymer chains rigidification and/or the chain entrance to the filler porosity [39].

Table 5. Glass transition temperature of various MMMs as a function of filler content.

Membrane	Filler content, %	Tg [°C]
Neat Matrimid	0	328.7 ± 4.6
MMM – ZIF-8	12	349.1 ±3.7
MMM – MIL-101	12	338.2 ± 1.5
MMM - MCM-41spheres	12	337.2 ± 1.7
MMM - silica-(ZIF-8) core-shell	12	338.7

In order to study thermal stability of the MMMs, the Thermo Gravimetric Analysis was performed and the loss of weight as a function of temperature was determined (Fig.8).

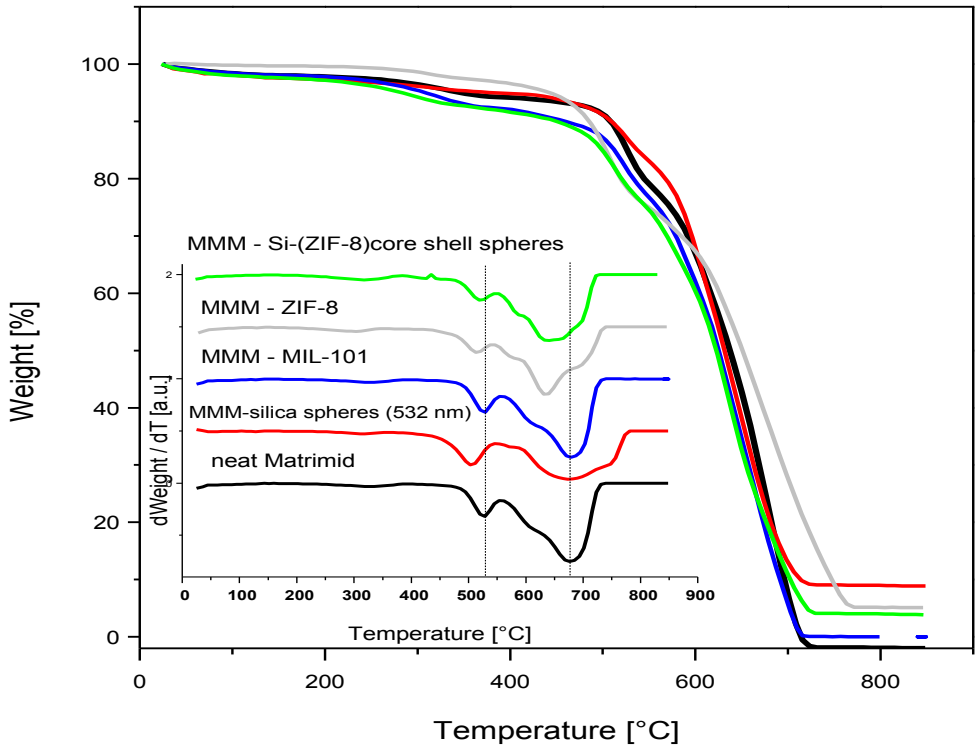

Figure 8. TGA weight losses versus temperature for the various membranes.
(The inset shows the corresponding derivatives).

TGA results show that there was no loss of weight up to 500 °C indicating that there was no solvent remaining in the membrane. Above this temperature, at around 520 °C, we can see the first peak that is responsible for the first degradation of the polymer while H_2, CO, CO_2 and CH_4 gases release from the sample. At 650 °C and higher there is a sharp decrease in weight indicating complete degradation of the polymer chain caused by the evolving of residual non-elementary carbon components, primarily N_2 [40]. The incorporation of different fillers into polymer phase did not improve the thermal stability of the membranes, the stability of MMMs was pretty much the same as in the case of neat Matrimid membrane.

4.3.2 Mixed matrix membranes containing 20 wt% of various fillers.

For the PV experiment MMMs were prepared with addition of 20 wt% of the following fillers: MCM-41 type silica spheres (size 3.1 μm), MCM-41 type silica spheres (size 530 nm), ZIF-8 (size 171 nm), commercial HKUST-1 (size 16 μm) and HKUST-1 synthesized in the laboratory (size 680 nm).

As we can see in the Table 6 membrane containing ZIF-8 sieves improved the permeability comparing to the results of membrane with 12 wt% of this MOF. Actually with a higher loading of ZIF-8, the nanoparticles formed agglomerates, but this MOF still shows good adhesion with the polymer. The nanoparticles in the matrix were in large aggregates, ranging up to micrometer in size (emphasized with yellow circles in Fig.9). Normally, poor dispersion creates paths for unselective transport of mixture components between the particles during permeation, resulting in increase in permeability and large decrease in selectivity [41]. And this hypothesis is confirmed by our results, where with increase of ZIF-8 loading from 12 to 20 wt% resulted in the increase in permeability from 0.24 to 0.31 kg/(m^2·h) while separation factor was downgraded from 386 to 79.

Table 6. PV performance of MMMs containing 20 wt% of various fillers.

Membrane	Filler type	Flux [kg/(m^2· h)]	Separation factor
neat Matrimid	no	0.24	260
MMM	HKUST-1 (16 μm)	0.25	283
MMM	ZIF-8	0.31	79
MMM	HKUST-1 (675 nm)	0.31	148
MMM	silica spheres (3.1 μm)	0.36	123
MMM	silica spheres (532 nm)	0.45	156

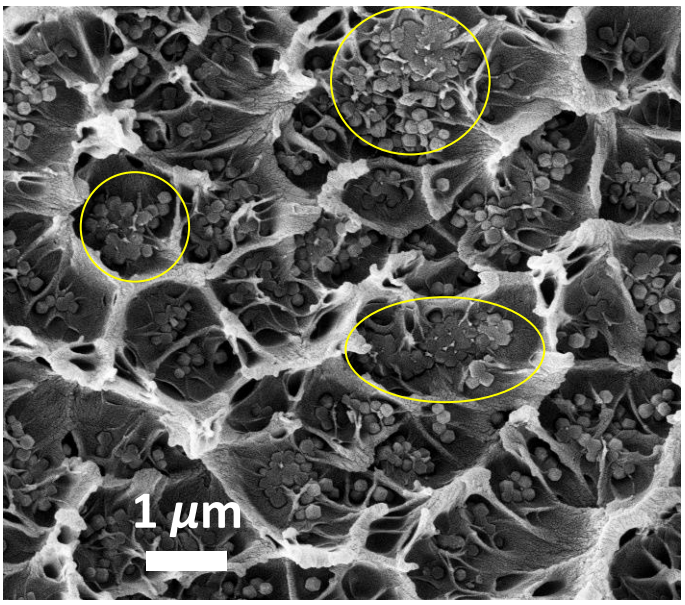

Figure 9. Cross section SEM image of MMM-(20 wt% ZIF-8)

Due to a significant enhancement of membrane permeability with an increase of filer loading, it was decided to use a higher loading of sieves in the further experiments. Also our results confirmed that the membranes that contain smaller size sieves have a higher permeability (Table 6) and this can be related to the fact that smaller particles yield more polymer/particle interfacial area and provide more opportunity to disrupt polymer chain packing and affect molecular transport. Thus it was concluded to use nano size particles for higher loading in the further experiments.

Unfortunately, membranes with content of silica spheres more than 20 wt% did not provide any improvement in separation, the membrane even got broken during the pervaporation test. The high loading of silica such as 30 and 40 wt% led to particles agglomeration and as a result formation of membranes with morphological defects. However in the case of 675 nm HKUST-1 crystals, the incorporation of high filler amounts was successful due to better compatibility of the MOF with the polymer. The pervaporation results of HKUST-1 loading into Matrimid up till 40 wt% are discussed in details in the section 4.3.3

4.3.3 Mixed matrix membranes containing HKUST-1

The permeability of the neat Matrimid membrane was improved in the presence of HKUST-1 particles when loaded with different amounts, i.e. 20, 30, 40 wt%. A number of membranes were tested in order to perform reproducibility and the average values of permeation flux and separation

factor are presented in the Table 7. In particular, four membranes containing 20 wt% of the filler and three membranes with 30 wt% were tested.

Table 7. PV performance of the MMMs with increasing HKUST-1 loading.

HKUST-1 content, [%]	Permeation flux, [kg/(m^2·h)]	Separation factor
0	0.24 ± 0.03	260 ± 28
20	0.31 ± 0.09	148 ± 28
30	0.41 ± 0.08	245 ± 29
40	0.43	208

As can be seen (Fig.10) with highest HKUST-1 loading a significant enhancement in the flux was observed with some trade off in separation factor. Increase in permeation flux can be attributed to both polymer plasticization effect in the presence of water and hydrophilic nature of the MOF which can pass water molecules much more freely than polymer matrix.

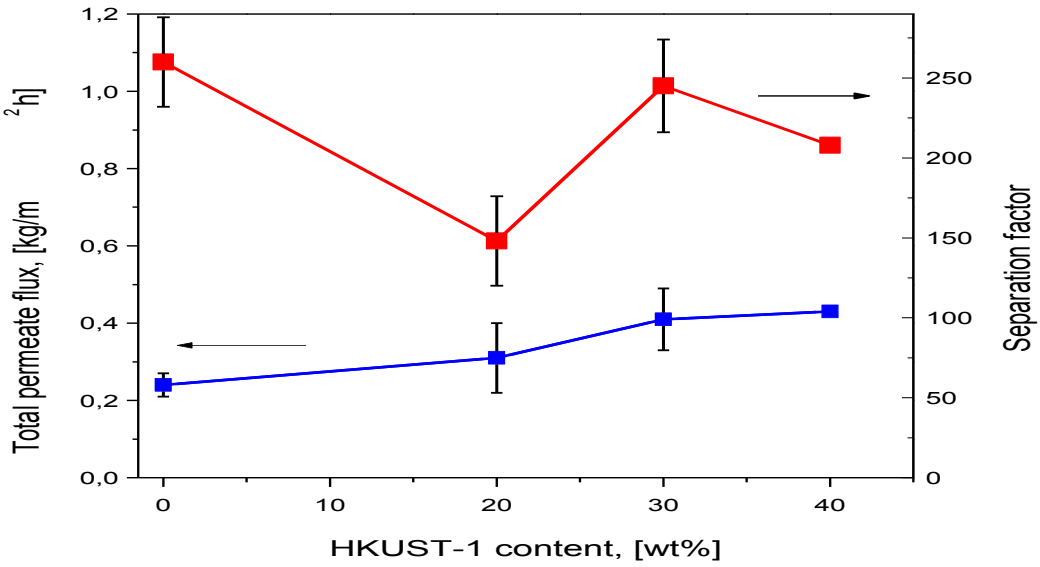

Figure 10. PV flux and separation factor of the membranes as a function of HKUST-1 content in Matrimid.

In overall, the compatibility of HKUST-1 and Matrimid seems good (Fig.11) due to organic nature of both materials, a homogeneous membranes were prepared with the MOF content of 20 and 30 wt%. But the improvement in flux however is less than was expected and may be due to issues of chain rigidification or particle agglomeration. We can clearly see (Fig.11 c) that with a higher loading of HKUST-1 such as 40 wt% particle agglomeration takes place, resulting in formation of non-selective voids. Also chain rigidification may play an important role in

determining the overall performance. As shown in the Table 8 the glass transition temperature of mixed matrix membranes increased with HKUST-1 loading. Clearly, chain rigidification exists in MMMs as reported elsewhere [10, 13, 42] and this may affect the membrane performance.

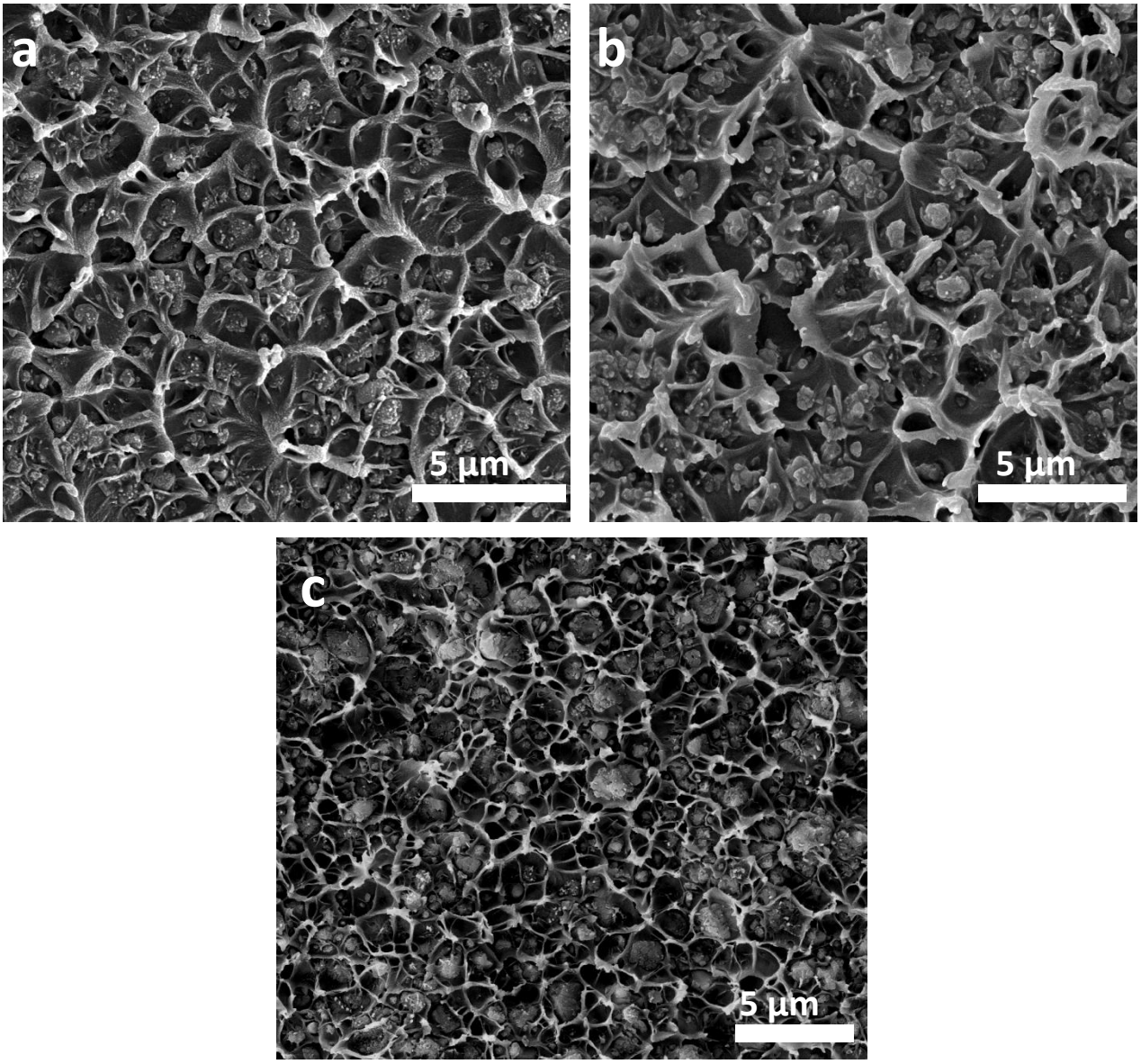

Figure 11. Cross section SEM images of MMMs containing HKUST-1 (a) 20 wt%; (b) 30 wt%; (c) 40 wt%.

As we already have mentioned before, with increasing the filler content in the MMM, the Tg increases as well (Table 8). It means that there is an increase of rigidity and restricted motion of the polymer chains due to interaction between polymer phase and MOF. Since there were no nonlinear changes in the Tg with increasing the loading of the filler, there were no disruption of physical cross links between the polymer chains [43].

Table 8. Glass transition temperature of MMMs as a function of HKUST-1 content.

Polymer	MOF type added	MOF loading [wt%]	Tg [°C]
Matrimid	-	0	328.7 ± 4.6
Matrimid	HKUST-1	20	348.6 ± 0.9
Matrimid	HKUST-1	30	350.1 ± 2.5
Matrimid	HKUST-1	40	358.2 ± 0.4

As shown in the Fig.12 the TGA curves of HKUST-1 powder and MMMs containing HKUST-1 consist of a few weight loss steps. At the initial period (around 100 °C) the weight loss is due to the evaporation of water molecules. After that the samples were not shown any significant weight change up to 320 °C for the HKUST-1 powder and 360 °C for the MMMs which are then gradually started to lose the weight. This shift of the temperature from 320 °C to 360 °C justifies the improvement of the filler stability. But the overall membrane stability is higher in the case on neat Matrimid compare to MMMs containing HKUST-1 and this can be justified by a catalytic effect of the copper in the MOF on the thermal degradation of the polymer. At 330 °C the weight change was observed (30%) due to decomposition of organic ligand, particularly BTC linker, and remained product was CuO [44].

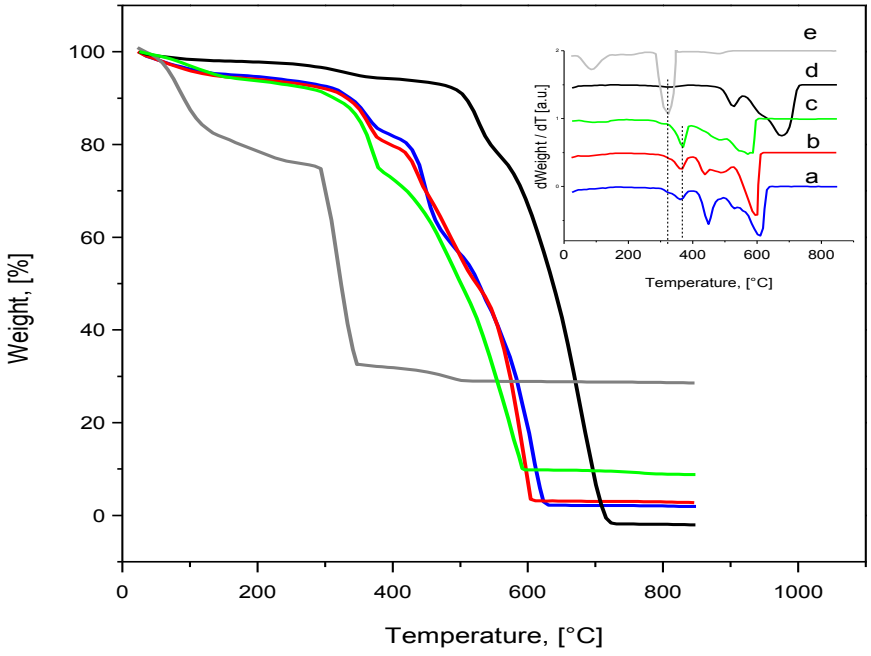

Figure 12. TGA weight losses versus temperature as a function of HKUST-1 loading: (a) 20 wt% HKUST-1; (b) 30 wt% HKUST-1; (c) 40 wt% HKUST-1; (d) neat Matrimid; (e) HKUST-1 powder. (The inset shows the corresponding derivatives)

Based on solution-diffusion mechanism, sorption characteristics of membranes play important roles in PV separation performance [15]. Major drawbacks of hydrophilic materials are its excessive swelling behavior resulting from the hydrogen bonding between the hydrophilic functional groups of the polymer and the water molecule, and water-soluble properties [45]. The degree of swelling of the neat Matrimid and MMMs containing HKUST-1 are presented in the Fig. 13.

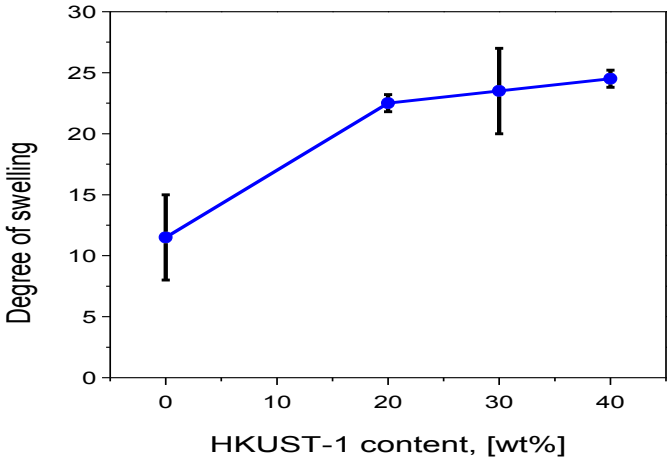

Figure 13. Degree of membrane swelling versus HKUST-1 content.

The MMMs swelling degrees are much greater than that of the neat Matrimid membrane. The incorporation of HKUST-1 nanoparticles enhances the water uptake into the membrane and this phenomena is confirmed by TGA curves (Fig.12) that shows that at temperature below 100 °C MMMs contain in their pores water molecules.

4.3.4 Mixed matrix membranes containing silica spheres MCM-41.

As was discussed before mesoporous silica spheres of nano-meter size compare to micro sized particles, embedded into polymer matrix, provide a better separation performance due to the higher interfacial area with the polymer. It can be seen in the Fig.14 that membranes with 12 and 20 wt% of the filler have a good distribution of silica particles, without apparent segregation of the spheres resulting in the formation of homogeneous films. Due to mesoporosity of silica particles, and taking into account that the cross sectional areas per chain of the most selective synthetic polymers are around 1 nm^2 or less, the polymer chains are able to penetrate into the pores of silica to give rise to a real homogeneous nanoporous composite, hence render a good adhesion between the fillers and polymer [13].

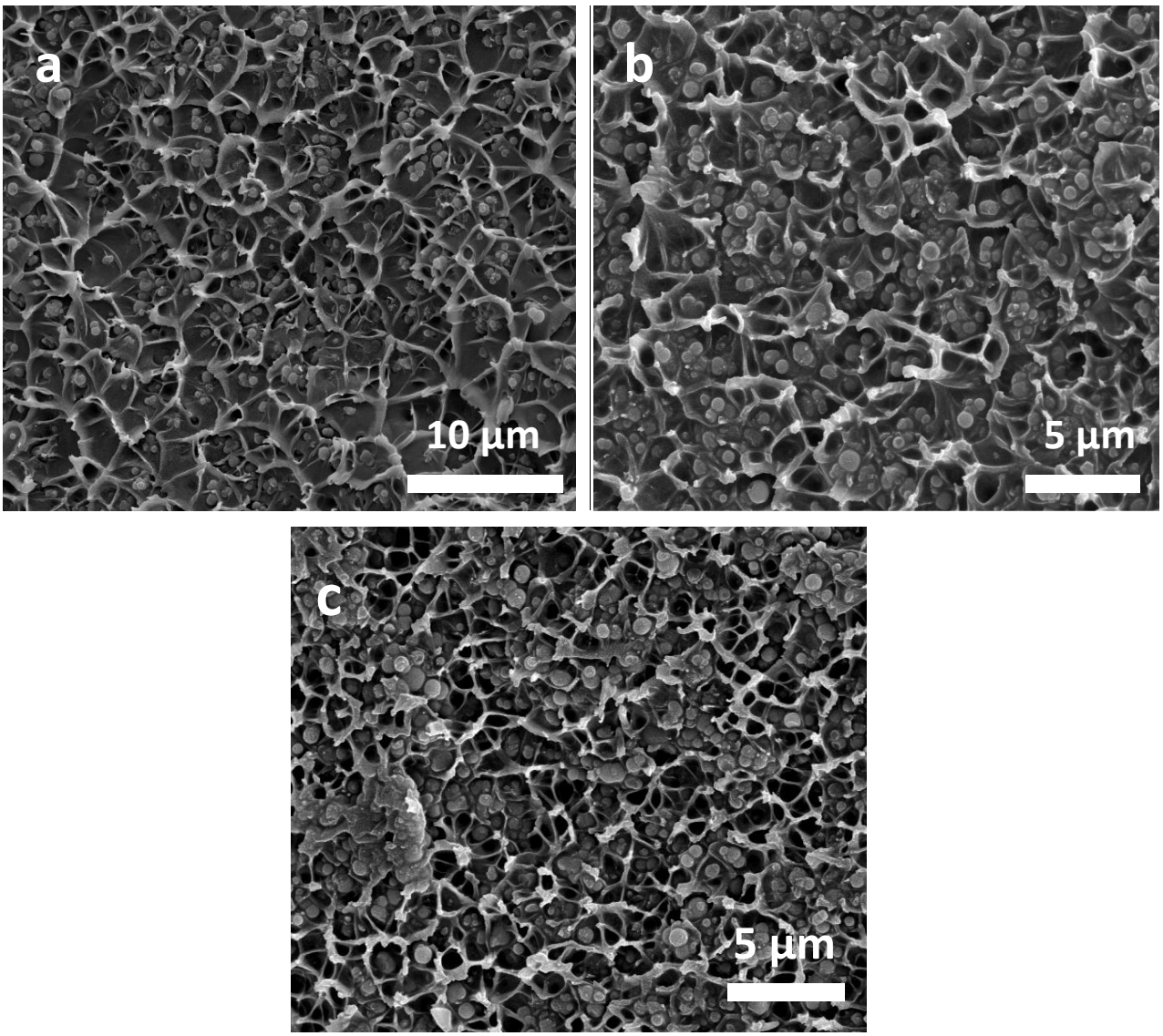

Figure 14. Cross section SEM images of MMMs containing silica spheres MCM-41

(a) 12 wt%; (b) 20 wt%; (c) 30 wt%.

However with increasing loading up to 30 wt% of the filler there was particle agglomeration leading to the formation of inhomogeneous membrane. With such a high amount of silica spheres the membrane lost its stability due to big particle agglomerates and as consequence the membrane was broken immediately under PV conditions.

With even more higher silica loading (40 wt%) it was not possible to prepare MMM due to the same phenomena as particles agglomeration and low amount of polymer around the spheres resulted in membrane cracks during the casting procedure. The reason of the agglomeration is the fact that unmodified nano-sized mesoporous silica has a higher surface area covered by hydrophilic silanol groups than microsized silica spheres. Consequently, the silica particles easily adhere to each other via hydrogen bonding and form irregular agglomeration in the polymer matrix [46]. So we can conclude that organic polymer did not show a good compatibility with high amount of

inorganic silica spheres even notwithstanding on the ability of polymer to penetrate into silica pores.

Nevertheless the use of spheres of 2-4 μm minimizes agglomeration and improves dispersibility because the spherical shape limits the contact between silica [13] but any way high loading of spheres leads to membrane damage under the separation conditions as was reported before [47] for gas separation applications.

The DSC analysis (Table 9) confirms the increase in polymer rigidity with increase of filler loading. By adding more filler, free volume of the polymer chain reduces since more and more connection of polymer chains to the filler surface and/or their entrance into the filler pores happen. These interactions between polymer chains and incorporated fillers restrict movement of the polymer chains and this causes Tg values of MMMs to be increased [48].

Table 9. Glass transition temperature of MMMs as a function of silica spheres MCM-41 content.

Polymer	**Filler loading, [wt%]**	**Tg, [°C]**
Matrimid	0	328.7 ± 4.6
Matrimid	12	337.2
Matrimid	20	347.7
Matrimid	30	358.2

Therefore the optimum loading of silica spheres into polymer matrix is 20 wt% which lead to the formation of homogeneous membrane with good separation properties.

4.4 ATR-FTIR characterization of various membranes.

The ATR-FTIR spectra of the membranes are shown in the Fig. 15. The absorbance of MMM containing HKUST-1 or silica spheres MCM-41are almost indistinguishable from the neat Matrimid membrane. The band at 2975 cm^{-1} is attributed to the C-H stretching of the methyl group. Peaks at 1780 and 1720 cm^{-1} are assigned to the symmetric and asymmetric stretching of the C=O groups of the imide. The peak at 1620 cm^{-1} is assigned to the benzophenone C=O stretching mode. The bands at 1515 and 1485 cm^{-1} are assigned to the aromatic stretching of the para-disubstituted phenyl group. The 1365 and 1090 cm^{-1} absorption bands are for the stretching modes of the C-N-C of the imide 5-membered ring [49].

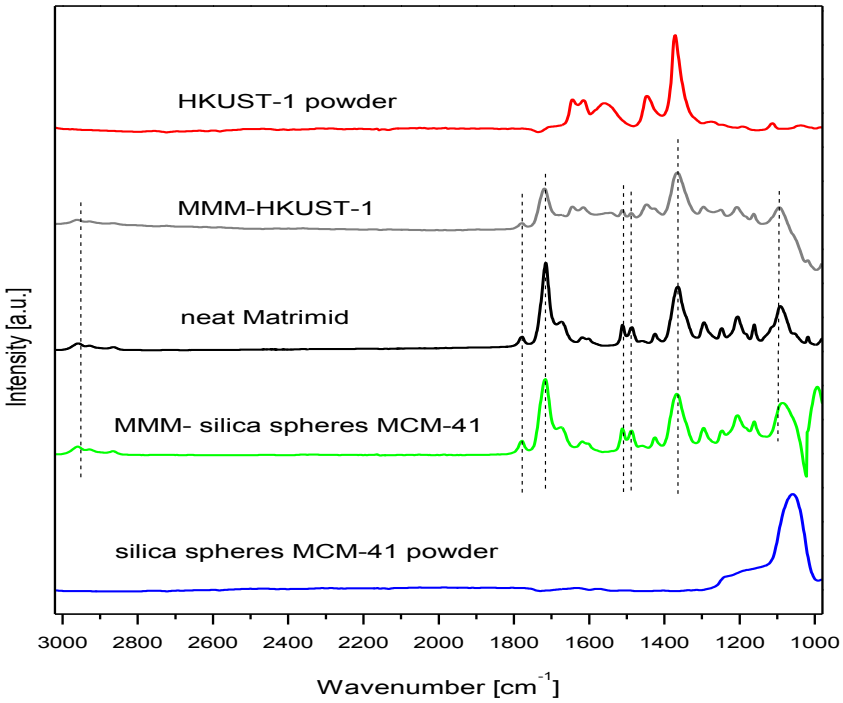

Figure 15. ATR-FTIR spectra of the neat Matrimid membrane and MMM containing 20 wt% of HKUST-1and MMM containing 20 wt% of silica spheres MCM-41.

The ATR-FTIR curve of the HKUST-1 powder shows two small peaks of around 1630 cm^{-1} that are assigned to ν (C=O) of the deprotonated benzene tricarboxylic acid [44]. Band around 1450 cm^{-1} is due to a combination of benzene ring stretching and deformation modes. Adsorption bands at 1570 and 1420 cm^{-1} are due to symmetric stretching vibrations of carboxylate groups and the symmetric vibrations centered at 1350 cm^{-1} [50, 51].

In the case of silica spheres MCM-41 powder characterization there is one significant peak at 1050 cm^{-1} that is corresponding to the SiO_2 characteristic bands due to vibrations of Si-O-Si bridges crosslinking the silicate network [52].

5. Conclusions.

The PV performance of the membranes strongly depends on the operating temperature of the system. We have prepared and tested a number of membranes based on neat Matrimid at two different temperatures which are 40 and 55 °C. We have observed that at higher temperatures the permeability of the membranes is much greater. However with increased temperature the selectivity of the membrane was decreased due to the thermal motions of polymeric chains that generate more free volume in the polymer matrix and facilitate absorption and diffusion of ethanol and water molecules. Since the first experiments showed higher permeation rate and faster steady state achievement at 55 °C, this temperature was fixed as the best for the rest of the PV experiments.

A number of MMMs were prepared containing different fillers and their different loadings into polymer matrix. The nature of the fillers used in this work and their pore size play an important role in distinguishing the molecules of ethanol/water mixture that needs to be separated. Increasing the amount of molecular sieves in the membranes led to a significant increase in permeability with the trade off in membrane selectivity.

The best results in terms of pervaporation performance showed mixed matrix membrane containing 12 wt% of silica spheres MCM-41 (size 530 nm). Compared to the neat Matrimid membrane, the PV flux of this MMM was improved from 0.24 to 0.44 kg/(m^2h) while separation factor was decreased from 260 to 229. Higher loading of silica spheres resulted in less flexible MMMs that were difficult to handle. In terms of stability of mixed matrix membranes with high loadings of MOFs and satisfying PV performance showed membranes containing HKUST-1 nanoparticles. We successfully prepared membranes with HKUST-1 loadings up to 40 wt% and tested them in dehydration of ethanol. A good separation properties showed membrane with 30 wt% of HKUST-1 where PV flux was improved from 0.24 (for neat Matrimid membrane) to 0.41 kg/(m^2h) without significant change in selectivity.

In order to prepare membranes free of defects, we performed fabrication of the membranes with controlled evaporation rate of the solvent by means of completely covered membranes with glass pale during the casting. It is believed that with controlled solvent evaporation rate there are uniform stresses that will minimize the formation of rigidified layer around the particles and hence will not affect their ability to perform separation.

In this research work it was confirmed that the use of molecular sieves with smaller particle size results in a better membrane performance. In particular, two types of sieves were used in this investigation, which are silica spheres MCM-41 of size 3.1 μm and 53o nm and HKUST-1 of size 16 μm and 680 nm. In this study, separation of ethanol/water mixture via PV, we observed that the use of smaller particles yield more polymer/particle interfacial area and provide more opportunity to

disrupt polymer chain packing and affect molecular transport and as consequence leads to an enhancement in permeability.

6. Recommendations for the future work

1. Pervaporation membranes show complicated behavior depending on many parameters such as operating temperature and feed composition. Therefore, in order to study mass transport of penetrants across the membrane under PV conditions it is recommended to perform PV experiment for the neat Matrimid membrane:
   - at temperature higher than 55 °C,
   - with different feed composition, for instance 20/80 wt%; 15/85 wt% and 4/96 wt% of water/etahanol mixture.

   Based on the different results of membrane performance, depending on operating temperature and feed composition, it will be possible to plot an upper bound limit line for the Matrimid membrane and therefore in the future it will be easier to compare the results of MMMs with the neat polymeric membrane.

2. To prepare neat Matrimid membranes and perform thermal pre-treatment in the vacuum oven for 24 hours at two different temperatures, for instance, 100 and 150 °C. And then study how different pre-treatment temperatures will affect the overall membrane performance. (In our experiments we treated all the membranes at 180 °C). According to Ansaloni and co-workers, membrane samples treated at 100 °C and higher definitely will be free of solvent, but different temperatures will lead to different glassy structure in the final films. In their study [19], they concluded that with increased temperature of thermal pre-treatment of the Matrimid membranes the permeability of gases was decreased. Hence, in dehydration of alcohols the Matrimid membranes may behave in the same way, i.e. the transport properties will be depended on the temperatures of membranes pre-treatment or, in the other words, will be related to changes in free volume and consequently density of the polymer matrix.

3. MMMs can be applied for dehydration of the other alcohols or even separation of organic/organic mixtures via pervaporation.

7. References

1. Lipnizki, F., R.W. Field, and P.K. Ten, *Pervaporation-based hybrid process: a review of process design, applications and economics.* Journal of Membrane Science, 1999. **153**(2): p. 183-210.
2. Jiang, L.Y., et al., *Polyimides membranes for pervaporation and biofuels separation.* Progress in Polymer Science, 2009. **34**(11): p. 1135-1160.
3. Peter D. Chapman, T.O., Andrew G. Livingston, K. Li., *Membranes for the dehydration of solvents by pervaporation.* Journal of Membrane Science, 2008. **318**: p. 5-37.
4. Tsai, H.A.L., L. D. Lee, K. R. Wang, Y. C. Li, C. L. Huang, J. Lai, J. Y., *Effect of surfactant addition on the morphology and pervaporation performance of asymmetric polysulfone membranes.* Journal of Membrane Science, 2000. **176**(1): p. 97-103.
5. Shao P., H.R.Y.M., *Polymeric membrane pervaporation.* Journal of Membrane Science, 2007. **287**: p. 162-179.
6. Robeson, L.M., *Correlation of separation factor versus permeability for polymeric membranes.* Journal of Membrane Science, 1991. **62**(2): p. 165-185.
7. Noble, R.D., *Perspectives on mixed matrix membranes.* Journal of Membrane Science, 2011. **378**(1-2): p. 393-397.
8. Mellot-Draznieks C.; Dutour, J.F., G., *Metal-Organic Frameworks: New Routes towards Hybrid Crystal Structures.* Chem. Int. Ed, 2004. **43**: p. 6290-6296.
9. Khan, N.A., et al., *Facile synthesis of nano-sized metal-organic frameworks, chromium-benzenedicarboxylate, MIL-101.* Chemical Engineering Journal, 2011. **166**(3): p. 1152-1157.
10. Gui Min Shi, T.Y., Tai Shung Chung, *Polybenzimidazole (PBI)/ zeolitic imidazolate frameworks (ZIF-8) mixed matrix membranes for pervaporation dehydration of alcohols.* Journal of Membrane Science, 2012. **415-416**: p. 577-586.
11. Xin-Lei Liu, Y.-S.L., Guang-Qi Zhu, Yu-Jie Ban, Long-Ya Xu, and Wei-Shen Yang, *An Organophilic Pervaporation Membrane Derived from Metal– Organic Framework Nanoparticles for Efficient Recovery of Bio- Alcohols.* Chem. Int.Ed, 2011. **50**: p. 10636-10639.
12. Yan Wang, S.H.G., Tai Shung Chung, Peng Na, *Polyamide-imide/polyetherimide dual-layer hollow fiber membranes for pervaporation dehydration of C1-C4 alcohols.* Journal of Membrane Science, 2009. **326**: p. 222-233.
13. Beatriz Zornoza, C.T., Joaquin Coronas, *Mixed matrix membranes comprising glassy polymers and dispersed mesoporous silica spheres for gas separation.* Journal of Membrane Science, 2011. **368**: p. 100-1009.
14. Semenova, S.I., H. Ohya, and K. Soontarapa, *Hydrophilic membranes for pervaporation: An analytical review.* Desalination, 1997. **110**(3): p. 251-286.
15. T. Khosravi, S.M., O. Bakhtiari, T. Mohammadi, *Mixed matrix membranes of Matrimid 5218 loaded with zeolite 4A for pervaporation separation of water–isopropanol mixtures.* Chemical Engineering Research and Design, 2012. **90**: p. 2353-2363.
16. Vollhardt, K.P.C.S., N. , *Organic Chemistry*. 5th ed. 2007, New York: W. H. Freeman.
17. Der-Jang Liaw, K.-L.W., Ying-Chi Huang, *Advanced polyimide materials: Syntheses, physical properties and applications.* Progress in Polymer Science, 2012. **37**(7): p. 907-974.
18. M.A. Aroona, A.F.I., T. Matsuurab, M.M. Montazer-Rahmatia, *Performance studies of mixed matrix membranes for gas separation: A review.* Separation and Purification Technology 2010. **75**: p. 229-242.
19. Ansaloni L., B.G.M., Mineli M., Sarti G.C., *Study of transport properties of matrimid polyimide: Effect of thermal history of physical aging.* Procedia Engineering, 2012(44): p. 840-842.

20. Qiu, W., et al., *Dehydration of ethanol-water mixtures using asymmetric hollow fiber membranes from commercial polyimides.* Journal of Membrane Science, 2009. **327**(1-2): p. 96-103.
21. Katharina Hunger , N.S., Harold B. Tanh Jeazet , Christoph Janiak, Claudia Staudt and Karl Kleinermanns *Investigation of Cross-Linked and Additive Containing Polymer Materials for Membranes with Improved Performance in Pervaporation and Gas Separation.* Membranes, 2012. **2**: p. 727-763.
22. Ravij Mahajan, W.J.K., *Factors Controlling Successful Formation of Mixed Matrix Gas Separation Materials.* Ind.Eng.Chem. Res, 2000. **39**: p. 2692-2696.
23. Koros W. J, M.Y.H., Shimidzu T., *Terminology for membranes and membrane processes (IUPAC recommendations).* Pure Appl Chem, 1996. **68**: p. 1479-1489.
24. Verweij, H., *Inorganic membranes.* Current Opinion in Chemical Engineering, 2012. **1**: p. 156–162.
25. Park, K.S., *Exceptional chemical and thermal stability of zeolitic imidazolate frameworks.* PNAS, 2006. **103**(27): p. 10186–10191.
26. Ryan P., M.E., Liren Xu et al., *A high-flux polyimide hollow fiber membrane to minimize foot print and energy penalty for CO2 recovery from flue gas.* Journal of Membrane Science, 2012: p. 302–313, 423–424.
27. Sara Sorribas, B.Z., Carlos Tellez and Joaquın Coronas, *Ordered mesoporous silica–(ZIF-8) core–shell spheres.* Chem. Commun, 2012. **48**: p. 9388–9390.
28. Skobelev, I.Y., et al., *Solvent-free allylic oxidation of alkenes with O2 mediated by Fe- and Cr-MIL-101.* Journal of Catalysis, 2013. **298**(0): p. 61-69.
29. Harold B. Tanh Jeazet, C.S.a.C.J., *Metal–organic frameworks in mixed-matrix membranes for gas separation.* Dalton Transactions, 2012. **41**(46): p. 13991–14212.
30. Schulz-Ekloff, G., J. Rathouský, and A. Zukal, *Mesoporous silica with controlled porous structure and regular morphology.* International Journal of Inorganic Materials, 1999. **1**(1): p. 97-102.
31. M. Manzano, V.A., C.O. Arean, F. Balas, V, Cauda, M. Colilla, M.R. Delgado, M. Vallet-Regi, *Studies on MCM-41 mesoporous silica fro drug delivery: effect of particle morphology and amine functionalization.* Chem. Eng., 2008. **137**: p. 30-37.
32. Jorge, M., N. Lamia, and A.E. Rodrigues, *Molecular simulation of propane/propylene separation on the metal–organic framework CuBTC.* Colloids and Surfaces A: Physicochemical and Engineering Aspects, 2010. **357**(1–3): p. 27-34.
33. Beatriz Zornoza, S.I., Carlos Tellez, Joaquin Coronas, *Mesoporous Silica Spheres - Polysulfone Mixed Matrix Membranes for Gas Separation.* Langmuir, 2009. **25**(10): p. 5903-5909.
34. Beatriz Zornoza, C.T., Joaquin Coronas, Jorge Gascon, Freek Kapteijn, *Metal organic framework based mixed matrix membranes: An increasingly important field of research with a large application potential.* Microporous and Mesoporous Materials 2013. **166**: p. 67-78.
35. Hyder, M.N., R.Y.M. Huang, and P. Chen, *Correlation of physicochemical characteristics with pervaporation performance of poly(vinyl alcohol) membranes.* Journal of Membrane Science, 2006. **283**(1–2): p. 281-290.
36. Mohd Ghazali Mohd Nawawi, A.N.S., Tan Gi Gi *Pervaporation of Ethanol-water using chitosanclay composite membrane* Jurnal Teknologi, 2008. **49(F)**: p. 179-188.
37. Vrentas J. S., D.J.L., *Diffusion in polymer—solvent systems. Reexamination of the free-volume theory.* Polymer Science: Polymer Physics, 1997. **15**(3): p. 403-416.
38. Theodore T. Moorea, W.J.K., *Non-ideal effects in organic–inorganic materials for gas separation membranes.* Journal of Molecular Structure 2005. **739**: p. 87-98.
39. Omid Bakhtiari, S.M., Tayebeh Khosravi and Toraj Mohammadi, *Preparation, Characterization and Gas Permeation of Polyimide Mixed Matrix Membranes.* Journal of Membrane Science and Technology, 2011. **1**(1): p. 1-8.

40. Barsema, J.N., et al., *Intermediate polymer to carbon gas separation membranes based on Matrimid PI.* Journal of Membrane Science, 2004. **238**(1-2): p. 93-102.
41. Joshua A. Thompson , K.W.C., William J. Koros , Christopher W. Jones, Sankar Nair, *Sonication-induced Ostwald ripening of ZIF-8 nanoparticles and formation of ZIF-8/polymer composite membranes.* Microporous and Mesoporous Materials 2012. **158**: p. 292-299.
42. Tai-Shung Chunga, L.Y.J., Yi Li, Santi Kulprathipanja, *Mixed matrix membranes (MMMs) comprimising organic polymers with dispersed inorganic fillers for gas separation.* Progress in Polymer Science, 2007. **32**: p. 483-507.
43. Jeroen Ploegmakers, S.J., Kitty Nijmeijer, *Mixed matrix membranes containing MOFs for ethylene/ethane separation-Part B: Effect of Cu3BTC2 on membrane transport properties.* Journal of Membrane Science, 2013. **428**: p. 331-340.
44. Feng, Y., et al., *Metal-organic frameworks HKUST-1 for liquid-phase adsorption of uranium.* Colloids and Surfaces A: Physicochemical and Engineering Aspects, accepted manuscript(0).
45. R.Y.M. Huang, R.P., G.Y. Moon, *Characteristics of sodium alginate membranes for the pervaporation dehydration of ethanol/water and isopropanol-water mixtures.* Journal of Membrane Science, 1999. **160**: p. 101-113.
46. Kim, S. and E. Marand, *High permeability nano-composite membranes based on mesoporous MCM-41 nanoparticles in a polysulfone matrix.* Microporous and Mesoporous Materials, 2008. **114**(1–3): p. 129-136.
47. Brian D. Reid, F.A.R.-T., Inga H. Musselman, Kenneth J. Balkus, Jr., and John P. Ferraris, *Gas Permeability Properties of Polysulfone Membranes Containing the Mesoporous Molecular Sieve MCM-41.* Chem. Mater., 2001. **13**(7): p. 2366-2373.
48. Qiao, X., T.-S. Chung, and R. Rajagopalan, *Zeolite filled P84 co-polyimide membranes for dehydration of isopropanol through pervaporation process.* Chemical Engineering Science, 2006. **61**(20): p. 6816-6825.
49. Ma. Josephine C. Ordonez, K.J.B.J., John P. Ferraris, Inga H. Musselman, *Molecular sieving realized with ZIF8/Matrimid mixed matrix membranes.* Journal of Membrane Science, 2010. **361**: p. 28-37.
50. Elisa Borfecchia, S.M., Diego Gianolio, Elena Groppo, Mario Chiesa, Francesca Bonino and Carlo Lamberti, *Insights into Adsorption of NH3 on HKUST‑1 Metal−Organic Framework: A Multitechnique Approach.* The Journal of Physical Chemistry, 2012. **116**: p. 19839−19850.
51. Wang, F., et al., *The controlled regulation of morphology and size of HKUST-1 by "coordination modulation method".* Microporous and Mesoporous Materials, 2013. **173**(0): p. 181-188.
52. Das, D.P., K.M. Parida, and B.K. Mishra, *A study on the structural properties of mesoporous silica spheres.* Materials Letters, 2007. **61**(18): p. 3942-3945.
53. Kujawski, W. and S.R. Krajewski, *Sweeping gas pervaporation with hollow-fiber ion-exchange membranes.* Desalination, 2004. **162**(0): p. 129-135.
54. M.H., M., *Basic principles of membrane technology*. 1996, Boston: Kluwer Academic. 557.
55. J.S. Vrentas, J.L.D., *Diffusion in polymer-solvent systems, I. Reexamination of the free-volume theory.* Journal Polymer Science, 1977. **15**: p. 403-416.
56. Wei Fen Guo, T.-S.C., *Study and characterization of the hysteresis behavior of polyimide membranes in the thermal cycle process of pervaporation separation.* Journal of Membrane Science, 2005. **253**: p. 13-22.
57. Shih-Hsiung Chen, R.-M.L., Cheng-Lee Lai, Mu-Ya Hung, Mei-Hui Tsai, Shih-Liang Huang, *Embedded nano-iron polysulfone membrane for dehydration of the ethanol/water mixtures by pervaporation.* Desalination, 2008. **234**: p. 221-231.
58. Widjojo, N. and T.-S. Chung, *Pervaporation dehydration of C-2-C-4 alcohols by 6FDA-ODA-NDA/Ultem (R) dual-layer hollow fiber membranes with enhanced separation*

performance and swelling resistance. Chemical Engineering Journal, 2009. **155**(3): p. 736-743.
59. Tai-Shung Chunga, W.F.G., Ye Liu, *Enhanced Matrimid membranes for pervaporation by homogenous blends with polybenzimidazole (PBI).* Journal of Membrane Science 2006. **271**: p. 221-231.
60. Kujawski, W., *Application of Pervaporation and Vapor Permeation in Environmental Protection.* Polish Journal of Environmental Studies 2000. **9**(1): p. 13-26.
61. S. Amnuaypanich, J.P., P.Phinyocheep, *Mixed Matrix Mebranes prepared from natural rubber/PVA seminterpenetrating polymer network (NR/PVA semi-IPN) incorporating with zeolite 4A for the pervaporation dehydration of water-ethanol mixtures.* Chemical Engineering Science, 2009. **64**: p. 4908-4918.
62. Robert Kreiter, D.P.W., Charles W.R. Engelen, Henk M. van Veen, Jaap F. Vente, *High-temperature pervaporation performance of ceramic supported polyimide membranes in the dehydration of alcohols.* Journal of Membrane Science, 2008. **319**: p. 126-132.
63. Jiang, L.Y., Chung, T.S. , *[beta]-Cyclodextrin containing Matrimid® sub-nanocomposite membranes for pervaporation application.* Journal of Membrane Science 2009. **327**: p. 216-225.

8. Annex.

Annex A: Fundamentals of pervaporation process.

Pervaporation is a separation process in which a binary or multicomponent liquid mixture is separated by partial vaporization through a membrane (Fig.16). During pervaporation, the feed mixture is in direct contact with one side of the membrane, while permeate is removed in the form of vapour state from the opposite side of the membrane into a vacuum and then condensed. The fraction of the feed that diffuses across the membrane is defined as the permeate, and the fraction that fails to pass through, the retentate.

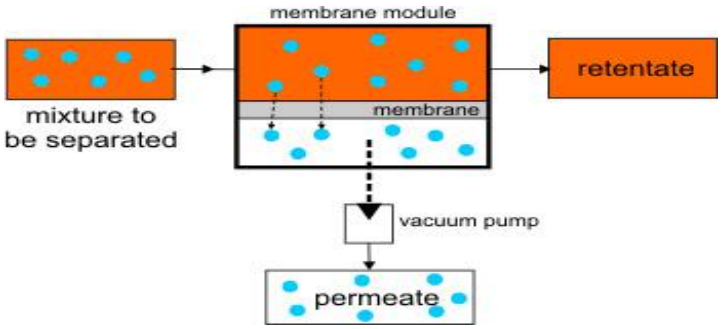

Figure 16. Schematic diagram of the pervaporation process [7].

In pervaporation, separation of mixture is obtained because of difference in the solubilities of the components in the membrane and diffusivities of these components through the membrane [53]. The diffusivity is a measure of the mobility of individual molecule passing through the voids between the polymeric chains in a membrane material. The solubility coefficient equals the ration of the dissolved penetrant concentration in the upstream face of the polymer to the upstream penetrant partial pressure [42]. Pervaporation process can be described by the solution-diffusion model which is mechanism of mass transport through non-porous membranes. The solution diffusion mechanism is based on the principle that the mixture component with higher solubility and higher diffusion rate permeates preferentially through the membrane, independent on the component size. This mechanism consists of three consecutive steps:

1. the permeant is dissolved in the feed side of the membrane;
2. the permeant diffuses though the membrane;
3. the permeant evaporates as vapour at the downstream side of the membrane [2].

When a PV membrane is in contact with a feed liquid mixture, it is generally believed that the thermodynamic equilibrium reaches instantly at the membrane-feed interface, therefore [5]:

$$\frac{c_m}{c_{feed}} = K \qquad (1)$$

where C_m and C_{feed} represent the concentrations of a species in the membrane surface and the feed, respectively, and K is the partition coefficient of a species between the membrane and the feed phase, which is a characteristic parameter dependent upon the interaction of the species in the membrane. Membrane transport is a rate controlling peocess, which is governed by the Fick's first law:

$$N = - D \frac{dC_m}{d\delta} \qquad (2)$$

where N is the permeation flux of the species through the membrane, D is the diffusion coefficient of the species in the membrane, and δ is the position variable. By introducing the partition coefficient K of the species at the membrane/feed and membrane/permeate interface, the concentrations of species in the faces of the membrane can be expressed in its concentrations in the feed and the permeate, respectively:

$$N = - DK \frac{\Delta C}{\delta} = \frac{DK}{\delta} \Delta C \qquad (3)$$

where both the diffusion (D) and the partition coefficient (K) are treated as constant, ΔC is the trans-membrane concentration and if ΔC is taken as driving force for the mass transport, the permeability then can be defined as following:

$P = DK$ (4)

And the ideal separation factor for species A and B can be defined as:

$$\alpha_B^A = \frac{P_A}{P_B} = \frac{D_A}{D_{BB}} \frac{K_A}{K_B} = (\alpha_B^A)_D \, (\alpha_B^A)_K \qquad (4)$$

However, when membrane is swollen or plasticized by transporting species, the interactions between polymer chains tend to be reduced, and the membrane matrix will therefore experience an icrease in the free volume. Solution-diffusion membranes feature free volume sites which cannot be occupied by polymer chains due to restricted motion and packing density of the polymer chains. The components are transported through the membrane by successive movement between the transient free volume gaps close to the feed side to those that are close to the permeate side due to thermal motion of segments of the polymer chains [54]. The fractional free volume (FFV) of polymers is defined as follows [5]:

FFV = specific free volume / polymer specific volume (5)

Increased volume lead to increased diffusion coefficients of the penetrants, the modified equations of the diffusion coefficient and the PV characteristics for binary mixture are defined in details in the following literature [5, 55].

Experimentally [2] the selectivity of the membrane can be expressed in terms of a separation factor, which is defined as:

$$\alpha_{A/B} = (Y_A/Y_B) / (X_A/X_B) \quad (5)$$

where X_A, X_B and Y_A, Y_B are the weight fractions of A (water) and B (ethanol) in the feed and permeate, respectively (A being the more permeative species).

And the total flux (J) through the membrane is defined as the total mass flow of all the permeating components through the membrane per unit area per unit time:

$$J= Q / (A*T) \quad (6)$$

where Q is total flux of permeate (kg), A is membrane area (m^2), T is interval time at steady state (hours).

Annex B. Characterization techniques

Gas chromatography (GC).

To determine the concentration of water and ethanol in the permeate, a Gas Chromatograph (Aligent Technologies, 7820A) was used. Samples were injected by the direct on-column injection technique. After calibration of GC was performed, each sample was analyzed 3-5 times.

Scanning electron microscopy

The geometrical characteristics and the morphology of the developed mixed matrix membrane was determined using scanning electron microscope (SEM). For the SEM studies membrane samples were immersed in liquid nitrogen and then fractured for preparing samples. Then the SEM samples were coated with gold using a sputter coater [56] and their cross sections were analyzed.

Differential scanning calorimetry

Differential scanning calorimetry (DSC) measurements were proceeded using a Mettler Toledo DSC822^e equipment to estimate the glass transition temperature of the MMMs with growing percentages of the filler. Small pieces of dried membranes (around 10 mg) were transferred to aluminum pans, which were hermetically sealed with aluminum covers. The samples were first scanned from room temperature to 400 ◦C with a heating rate of 10 °C/min. Two consecutive runs of this method were performed for each sample and the glass transition temperature (Tg) was determined from the middle point of the slope transition in the DSC curve. The reported Tg values are the average value based on the second runs of three samples [13].

Thermo-gravimetrical analysis

Thermo-gravimetrical analysis (TGA) was performed to determine the weight loss of all membrane samples and powders of some fillers as well as a function of temperature. Analysis was conducted using a Mettler Toledo TGA/SDTA 851^e. With this characterization technique we have studied the effect of fillers loading on thermal stability of the membranes. Samples (5 mg at least) were placed in 70 μL pans and then were heated in air flow up to 850 °C at a heating rate 10 °C/min.

Swelling measurement

The degree of swelling of membranes were determined in aqueous ethanol solution (10/90 wt% of water/ethanol) at 55 °C. The weight of dry membrane was first determined. After equilibrium with water/ethanol solution was reached, the fully swollen membrane was wiped tissue paper and weighed. The degree of swelling was calculated by the following equation [57]:

$$\text{Degree of swelling (\%)} = (W_{wet}-W_{dry}) / W_{dry} \times 100\%$$

Attenuated total internal reflection Fourier transform infrared spectroscopy (ATR-FTIR)

The ATR-FTIR characterization technique is needed to analyze the chemical structure changes of membranes with different fillers loading. The characterization of the membranes was performed on a Bruker Vertex 70 FTIR spectrometer equipped with a deuterated triglycine sulfate (DTGS) detector and a Golden Gate diamond ATR accessory .Spectra were recorder in the 4000-600 cm^{-1} wavenumber range. Data evaluation and spectra simulation were performed with OPUS software from Bruker Optics.

Brunauer-Emmett-Teller (BET) specific surface area

The BET specific surface areas of the fillers were measured from the adsorption branches in the relative pressure range of 0.05-0.25. The nitrogen adsorption-desorption isotherms of the fillers were measured at 77 K using a porosity analyzer (TriStar 3000, Micromeritics Instrument Corp.) All the samples were outgassed with a heating rate of 10 °C/min until 150-300 °C depending on the molecular sieve type and then maintained for 8 hours.

Annex C. Presentation of the steady state achievement of the MMMs containing 12 wt% of various fillers.

Fig.17 shows that mostly all of the MMMs achieved steady state of the system at 55 °C.

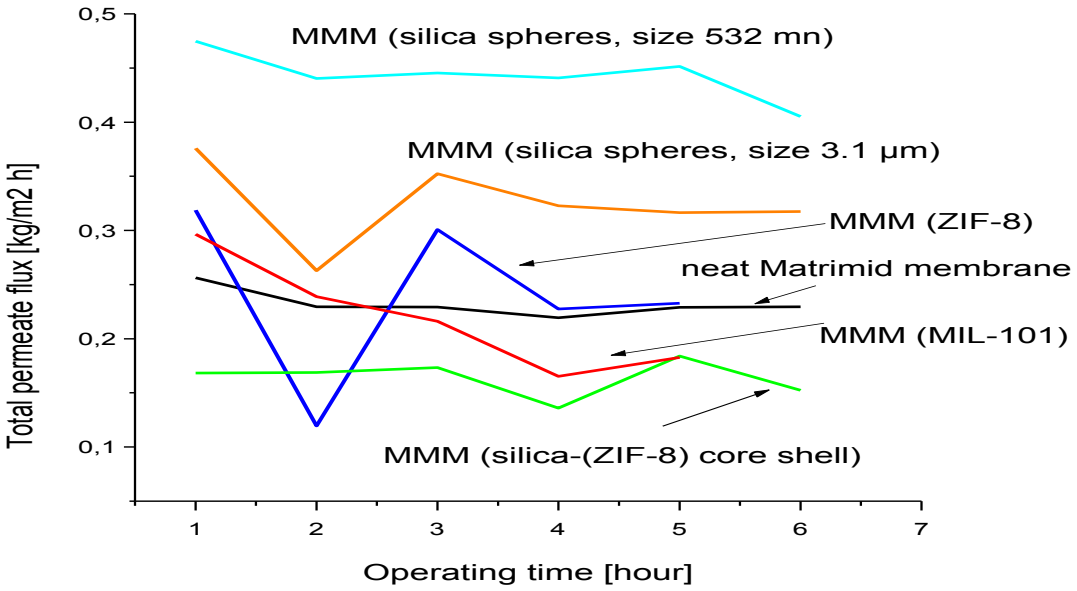

Figure 17. Total PV flux versus operating time at 55 °C

Annex D: TGA results of mixed matrix membranes containing 20 wt% of various fillers.

TGA curves of MMMs are depicted in the Fig.18, from where it can be seen that MMM containing HKUST-1 nanoparticles is less stable compare to the neat Matrimid membrane, the first structure degradation starts after 300 °C while a neat Matrimid is stable till 500 °C. However the rest of MMMs have stability similar to the neat membrane.

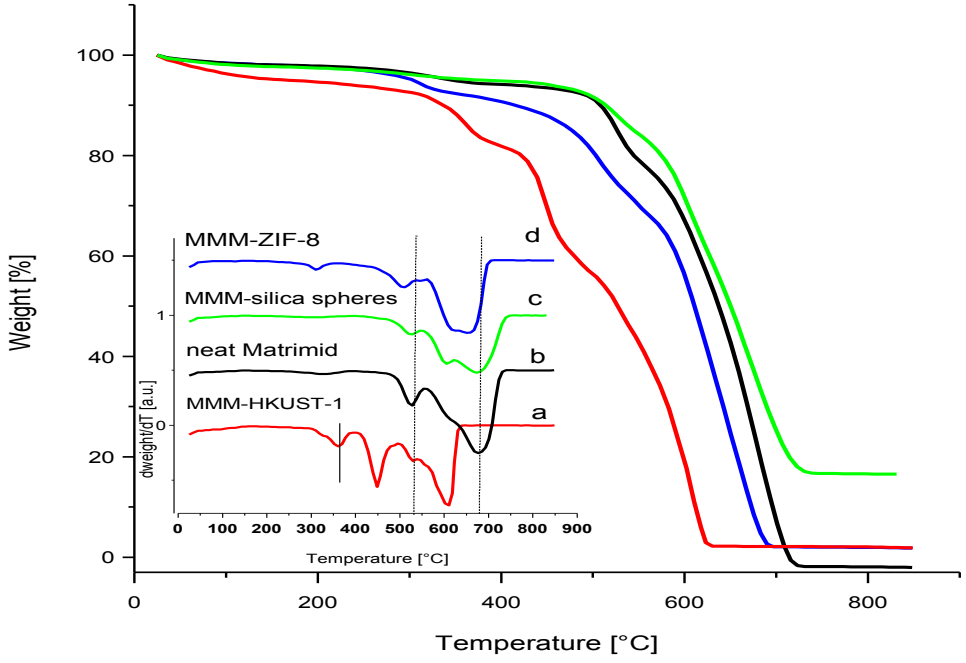

Figure 18. TGA weight losses versus temperature for the MMMs containing 20 wt% of various fillers.

(The inset shows the corresponding derivatives).

Annex E. Summary of the all performed experiments

All the results of pervaporation experiments are presented in Table 10, from where the membrane performance can be seen as a function of filler type and its amount in the polymer phase.

Table 10. MMMs for water/ethanol separation via pervaporation.

Membrane	Filler loading, [wt%]	Temperature, [°C]	Separation factor	Total permeate flux, [kg/(m^2 h)]
neat Matrimid 5218	No	40	0.19 ± 0.01	317 ± 25
neat Matrimid 5218	No	55	0.24 ± 0.03	260 ± 28
MMM-ZIF-8	12	55	0.24	386
MMM-ZIF-8	20	55	0.3	79
MMM-(silica-ZIF-8) core Shell	12	55	0.16	115
MMMM-MIL-101	12	55	0.21	709
MMM-silica spheres (3.1 μm)	12	55	0.32	206
MMM-silica spheres (3.1 μm)	20	55	0.36	123
MMM-silica spheres (532 nm)	12	55	0.44	229
MMM-silica spheres (532 nm)	20	55	0.45	156
MMM-HKUST-1 (16 μm)	20	55	0.25	283
MMM-HKUST-1 (675 nm)	20	55	0.31 ± 0.09	148 ± 48
MMM-HKUST-1 (675 nm)	30	55	0.41 ± 0.08	245 ± 29
MMM-HKUST-1 (675 nm)	40	55	0.43	208

Based on our results we can conclude that in separation process there is a strong inverse relationship between PV flux and separation factor of the membrane. Some of the MMMs that we have prepared and tested showed a significant improvement in PV flux, compare to the neat Matrimid membrane, and some of MMMs enhanced selectivity of the membrane without big changes in PV flux. The balance between PV flux and separation factor showed MMM containing 30 wt% of HKUST-1. The selectivity of the MMMs even can be enhanced by improving the

polymer-filler interface. And the incorporation of hydrophilic molecular sieves in a polymer matrix with high separation performance can be potentially commercialized in the case of overcoming durability problems of MMMs.

Annex F: Literature review of alcohol dehydration via pervaporation

Table 11. Dehydration of alcohols with different types of membranes.

Membrane	Mixture	Feed composition [wt%]	T, [°C]	Flux [kg/(m^{2}h)]	Separation factor	Ref.
6FDA-ODA-NDA/Ultem dual layer hollow fiber	Water/ EtOH	15/85	60	0.464	200.27	[58]
Torlon 4000TF hollow fiber	Water/EtOH	5/95	60	0.015	500-700	[12]
PAI/PEI dual-layer hollow fiber	Water/EtOH	15/85	60	0.659	50	[12]
Matrimid +PBI (blending and annealing)	Water/tert-butanol	15/85	25	0.42	1410	[59]
Matrimid hollow fiber (annealed)	Water/EtOH	15/85	45	0.15	132	[20]
Polyamide-6	Water/EtOH	30/70	80	1,15	2	[60]
NR/PVA semi-IPN + Zeolite 4A(40wt%)	Water/EtOH	10/90	30	0.33	2000	[61]
PBI/ZIF-8 (33.7 wt%)	Water/EtOH	15/85	60	0.99	10	[10]
Ceramic supported Matrimid	Water/n-buthanol	5/95	95	1.5	57	[62]
Matrimid/zeolite 4A (15 wt%)	Water/IPA	10/90	30	0.021	29.99	[15]
Matrimid/Beta cyclodextrin (10 wt%)	Water/IPA	14/86	22	0.18	22	[63]
Matrimid MgO (15 wt%)	Water/IPA	10/90	100	-	2000	[15]

Where : EtOH is ethanol; IPA is isopropanol; 6FDA-ODA-NDA is a polyimide polymer; Torlon is a polyamide-imide; PAI/PEI is a polyamide-imide / polyetherimide; NR/PVA semi-IPN is Natural Rubber/ PolyVinylAlkohol seminterpenetrating polymer network.